## Petrogenesis of the Pleistocene Tronador Volcanic Group, Andean Southern Volcanic Zone

Mauricio Mella Departamento de Geología, Universidad de Chile, Casilla 13518, Correo 21, Santiago, Chile

mauromella@esfera.cl

\*Present address: Instituto de Geociências, Centro de Pesquisas Geocronológicas, Rua do Lago 562, Cidade Universitaria, CEP 05508-080, São Paulo, Brasil

Jorge Muñoz Servicio Nacional de Geología y Minería, Oficina Técnica Puerto Varas, La Paz 406, Puerto Varas, Chile

jmunoz@sernageomin.cl

Mario Vergara Departamento de Geología, Universidad de Chile, Casilla 13518, Correo 21, Santiago, Chile

mariover@cec.uchile.cl

Erik Klohn Los Barbechos 479, Departamento 912, Las Condes, Santiago, Chile

eklohn@vtr.net

Lang Farmer Department of Geological Sciences, University of Colorado, Boulder, CO 80309-0399, USA Charles R. Stern

farmer@cires.colorado.edu sternc@colorado.edu

## **ABSTRACT**

The Tronador Volcanic Group (TVG) is located in the transition between the central and southern segment of the Andean Southern Volcanic Zone (SVZ), ≈50 km to the east of the current volcanic front. The TVG includes, from older to younger, the deeply eroded Early Pleistocene Garganta de Diablo unit (GDU; ≈1.3 Ma) and Steffen volcanic complex (SVC), the Middle Pleistocene Tronador Volcanic Complex (TVC; <1.0 Ma to ≈300 ka), as well as the post-glacial Fonck monogenic volcanic cone. Temporal petrochemical variations observed for older compared to younger samples from the TVG are similar to differences occurring across the active southern SVZ arc, from the current volcanic front to centers east of the front, and consistent with decreasing input of slab-derived fluids, and consequently decreasing percent of partial melting of the mantle source of the TVG. Relatively depleted (K<sub>2</sub>O<0.96 wt %; Rb<26 ppm; La<14.6 ppm) Group I basalts and basaltic andesites, and medium-K more differentiated rocks, were erupted to form the GDU and SVC during the Early Pleistocene. These have Ba/La>20 similar to the current volcanic front, but higher La/Yb and lower Yb, consistent with their genesis by 10% partial melting of subarc garnet-peridotite mantle, followed by 20% fractional crystallization involving olivine, clinopyroxene and plagioclase. Younger TVC Group I basic rocks have similar Ba/La, but higher Yb, and were generated by slightly lower degrees (7%) of partial melting in shallower garnet-free mantle. Beginning in the Middle Pleistocene (≈500-300 ka, Tronador II and III units of the TVC) relatively enriched (K<sub>2</sub>O>0.96 wt %; Rb>31 ppm; La>20 ppm) Group II basalts, with geochemical characteristics similar to volcanic centers east of the current volcanic front (Ba/La<20), were erupted together with Group I basalts. The generation of Group II rocks are consistent with 5% partial mantle melting in drier and shallower plagioclase-bearing mantle modified by less fluids derived from the subducted slab than involved in the generation of Group I rocks. Although these petrochemical changes were gradual, the relative volume of magma erupted across this region of the SVZ arc changed in the late Middle Pleistocene, after ≈300 ka, with the nearly complete termination of volcanic activity in the TVG and growth of Osorno and Calbuco volcanoes along the current volcanic front at this latitude.

Key words: Andean volcanism, Magma genesis, Partial melting, Fractional crystallization, Quaternary.

## **RESUMEN**

Petrogénesis del Grupo Volcánico Pleistoceno Tronador, Zona Volcánica Sur de los Andes. El Grupo Volcánico Tronador (GVT) se ubica en la zona de transición entre el segmento central y el segmento sur de la Zona Volcánica Sur (ZVS) de los Andes, ca. 50 km al oriente del frente volcánico actual. El GVT incluye, desde más antiguo a más joven, al complejo volcánico Steffen (CVS) y la unidad Garganta del Diablo (UGD; ≈1,3 Ma), ambos profundamente erosionados y edificados en el Pleistoceno Inferior, al complejo volcánico Tronador, construido en el Pleistoceno Medio (CVT; <1,0 Ma - ≈300 ka), y El cono monogénico postglacial Fonck. Las variaciones petrogenéticas temporales detectadas desde las rocas más antiguas hasta las más jóvenes son similares a las observadas a lo ancho del arco volcánico activo de la SVZ, desde los centros del frente volcánico hasta aquellos ubicados detrás del frente, y son consistentes con una disminución del aporte de fluidos derivados desde la placa subductada, con la consecuente disminución del porcentaje de fusión parcial de la fuente de los magmas. Los basaltos y andesitas basálticas relativamente empobrecidos (K,O<0,96 %; Rb<26 ppm; La<14,6 ppm) del Grupo I, y los miembros más diferenciados con contenidos medios de potasio, formaron los CVS y la UGD durante el Pleistoceno Inferior. Estas rocas tienen razones Ba/La>20 similares a aquellas del frente volcánico actual, pero mayor razón La/Yb y menor contenido de Yb, consistentes con 10% de fusión parcial de manto astenosférico de tipo peridotítico con presencia de granate, seguido por 20% de cristalización fraccionada de olivino, clinopiroxeno y plagioclasa. Por su parte, las rocas básicas más jóvenes del CVT, también agrupadas en el Grupo I, tienen similar razón Ba/La, más alto contenido de Yb y fueron generadas por un porcentaje menor (7%) de fusión parcial de manto astenosférico libre de granate, a una profundidad menor que las anteriores. En el Pleistoceno Medio (≈500-300 ka, las unidades Tronador II y III del CVT), basaltos relativamente enriquecidos (K<sub>2</sub>O>0.96%; Rb>31 ppm; La>20 ppm), agrupados en el Grupo II, con características geoquímicas similares a los centros volcánicos al este del frente volcánico actual (Ba/La<20), fueron generados en conjunción con basaltos del Grupo I. La generación de los magmas formadores de los basaltos del Grupo II es consistente con 5% de fusión parcial de manto más seco y con presencia de plagioclasa, a una menor profundidad y con menor participación de fluidos derivados desde la placa subductada, en comparación con los basaltos del Grupo I. Aunque estos cambios petrogenéticos serían graduales, el volumen relativo de magma eruptado a lo ancho del arco volcánico de la ZVS, a estas latitudes, cambió en el Pleistoceno Medio alto (después de ≈300 ka), con la completa extinción de la actividad del CVT y el inicio de la construcción de los volcanes Osorno y Calbuco en el frente volcánico actual.

Palabras claves: Volcanismo Andino, Genésis de magmas, Fusión parcial, Cristalización fraccionada, Cuaternario.

## INTRODUCTION

The Tronador Volcanic Group (TVG; Fig. 1) is located in the Andean Southern Volcanic Zone (SVZ; Stern, 2004), which extends from the intersection of the aseismic Juan Fernández ridge (33°S) to the Península de Taitao triple junction (46°S). The SVZ has been divided into four segments based on both tectonic and petrochemical features. The TVG occurs at the transition between the central segment (CSVZ, 37°-41°5'S) and the southern segment (SSVZ, 41°5'-46°S), in both of which the dominant rock types are basalts and basaltic andesites, while andesites, dacites and rhyolites are volumetrically less significant (Stern *et al.*, 1976; Futa and Stern, 1988; López-Escobar *et al.*, 1993, 1995a and b).

The TVG is located along the Chile-Argentina border, ≈50 km east of the current volcanic front

(Fig. 1). Pliocene and Quaternary evolution of the Andean volcanic arc at the latitude of the TVG, as well as elsewhere in the SVZ, involved either changes in the location of the volcanic front (Muñoz and Stern, 1988, 1989; Stern, 1989), or changes in the amplitude of volcanic activity in different portions of the volcanic arc without changing the present day location of the volcanic front (Lara et al., 2001). Chronologic and petrochemical information for the TVG suggests that significant variations occurred during its evolution, with changes in magma compositions from volcanic front type volcanism during the Early Pleistocene to behind the front type arc volcanism during the Middle Pleistocene. Previously, such geochemical changes were described only spatially, for magmas erupted along compared to behind the volcanic arc front, from

west-to-east across northeast (for example, Callaqui-Copahue and Osorno-La Picada-Puntiagudo) and northwest (for example, Puyehue-Cordón Caulle and Villarrica-Quetrupillán-Lanín) oriented geological structures, which play an important role in controlling the locations of volcanic

centers in both the CSVZ and SVZZ (López-Escobar et al., 1995b). As a consequence, the chronologic and petrochemical data for the TVG are relevant to understanding both the temporal evolution of the Quaternary volcanic arc as well as the spatial transition between the CSVZ and SSVZ.

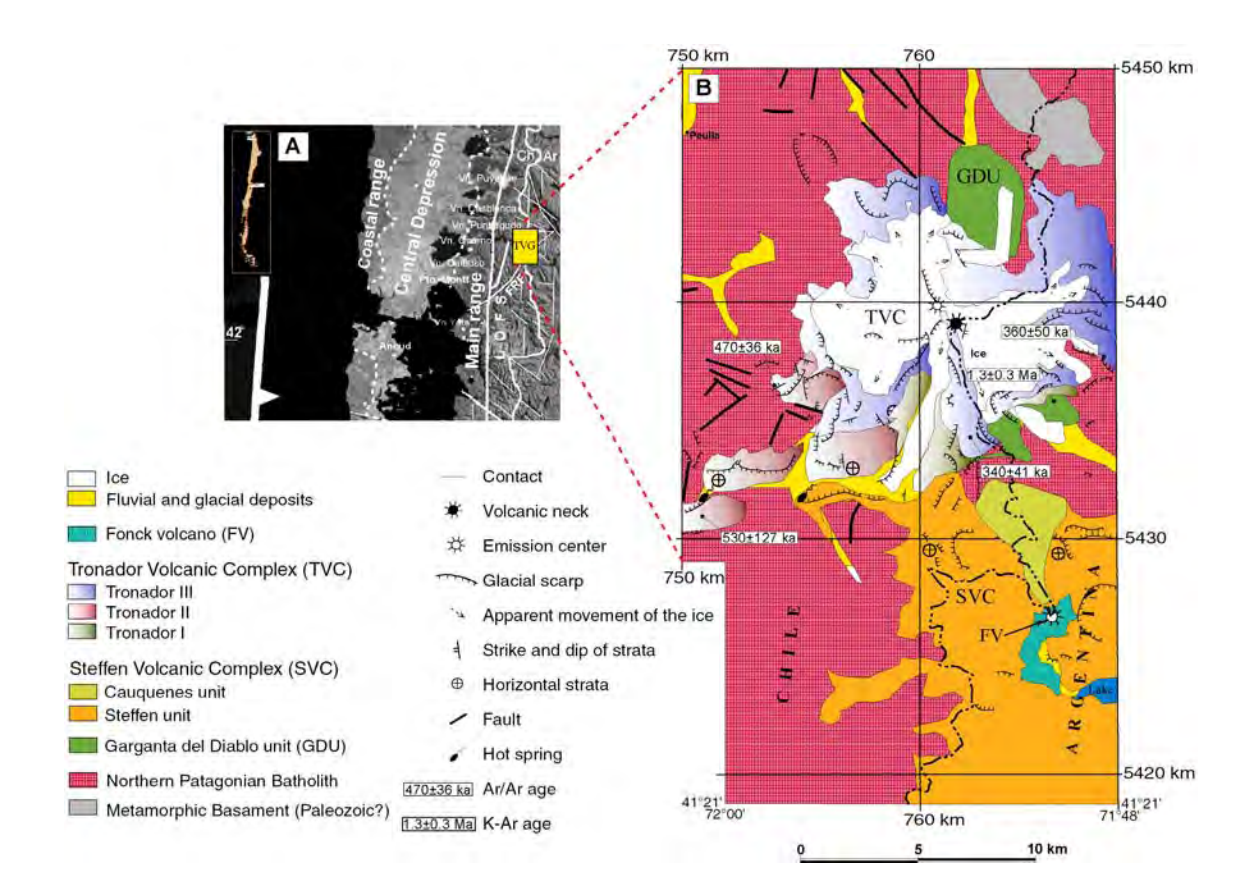


FIG. 1. A- Landsat image showing location of the Tronador Volcanic Group (TVG), volcanoes along the current volcanic front and other morphologic and structural features in this segment of the Andes; B- geological sketch of the TVG and location of dated samples (modified from Mella et al., 2003a). LOFS: Liquiñe-Ofqui fault system (Cembrano et al., 1996), FRF: Fiordo de Reloncaví Fault.

## **VOLCANIC COMPLEXES AND UNITS**

The basement for the TVG is formed by an uplifted block of Upper Cretaceous and Miocene granodiorites and diorites along the eastern edge of the Northern Patagonian Batholith, and minor undifferentiated metamorphic rocks (SERNA-GEOMIN-BGRM, 1985; Lavenu and Cembrano,

1999). The names and ages of the different stratigraphic units of the TVG have been controversial since the pioneering geological work of Steffen (1910, 1947). Previous proposals include: interglacial age Tronador Series (Ljungner, 1931; Larsson, 1940); Late Tertiary Mafic Effusive Series

(Aguirre and Levi, 1964); Early Pleistocene (Dessanti, 1972) or pre-Pleistocene (R. Greco¹) Tronador Formation; Plio-Pleistocene Glaciated Volcanic Rocks of the Upper Tertiary-Quaternary Volcanic and Sedimentary Series (Moreno and Parada, 1976); Miocene Collón Curá Formation (F. González-Bonorino²); Late Pliocene (K-Ar age of 3.2±2.0 Ma, Rabassa and Evenson, 1996; Rabassa *et al.*, 1987); and Plio-Pleistocene (Giacosa and Heredia, 2001).

In this paper, the TVG is divided into three main Pleistocene volcanic complexes/units related to a similar number of extinct and partially eroded volcanic centers. From older to younger they include the Garganta del Diablo unit (GDU) and the Steffen (SVC) and Tronador (TVC) volcanic complexes. The TVG also includes the monogenic Fonck volcano, which is postglacial and probably Holocene in age.

## **GARGANTA DEL DIABLO UNIT**

The GDU is formed by a sequence of dacitic lava flows and pyroclastic deposits with light brown color related to weak weathering. In the valley with this name (Fig. 2), the sequence includes two dacitic flows and related breccias. The lower flow has columnar jointing. The upper one is cut by northeast to northwest trending feeder dykes and disconformably covered by the Tronador I unit of the TVC (Fig. 2). The glacial erosion affecting the underlying granitic basement and the presence of fluvioglacial deposits below the lower columnar jointed dacite lava flow suggest that this unit was erupted during an intraglacial time period.

## STEFFEN VOLCANIC COMPLEX

This volcanic complex, which is located approximately 4 km to the south of the TVC summit (Fig. 1), fills an old glacial valley carved into both the granitic basement and the GDU. Its deep erosion and stratigraphic position confirm that the SVC is older than the TVC. The SVC is formed by, at least, two units, here named the Steffen and Los Cauquenes units. The former is the most extensive and forms a subhorizontal sequence, dipping slightly to the west, which includes columnar jointed olivine basalts and basaltic andesites, pyroclastic flows, lahars and related deeply eroded volcanic necks. Los Cauquenes unit has a more reduced extension

(<8 km²) and includes flow wrinkled basaltic andesite lavas deposited in a glacial valley carved into the Steffen unit. Los Cauquenes unit could have formed from a monogenic cone during an intraglacial time period.

## TRONADOR VOLCANIC COMPLEX

The TVC forms the partially eroded Tronador stratovolcano, which is the most prominent geographic feature in the area, with an altitude of 3,554 m a.s.l. and more than 225 km² in area. It has been divided into three main units, Tronador I, II and III (Figs. 1-3).

## **TRONADOR I UNIT**

This unit disconformably covers the GDU and is itself almost entirely covered by the Tronador II and III units. It constitutes the base of the Tronador volcanic complex (Figs. 1 and 2) and is formed by a repetitive sequence of basaltic to andesitic lava flows and pyroclastic and laharic deposits.

## TRONADOR II UNIT

This unit is divided into two main subunits named the Río Blanco Basalts and La Veranada stratigraphy (Fig. 4). The Río Blanco Basalts are restricted to an old glacial valley carved in the granitic basement on the Chilean side of the volcano. The lower part of this sequence includes a massive polimictic lahar and debris flows. The upper section is mainly formed by approximately 100 m of meter to decimeter thick columnar jointed olivine basalts with large plagioclase phenocrysts (1-2 cm in size), as well as basaltic andesite lava flows, both interbedded with phreatomagmatic flows (basal surge type) and lahars. Locally, lava flows with basal autobreccias (in part pseudo-pillow lavas), large oriented plagioclase phenocrysts, and partially palagonitized sideromelano and fiberpalagonite (Mella et al., 2003b), are interbedded with phreatomagmatic basal surge deposits. La Veranada stratigraphy is restricted to the western portion of the TVC and fill a hanging glacial valley carved into the granitic basement (Fig. 3). This sequence includes basaltic lava flows in the lower section and andesitic lava flows in its upper portion, interbedded with lahars, debris flows, tuffs and hyalotuffs.

<sup>1 1975.</sup> Geología de la hoja 40 a, 'Monte Tronador' (Inédito). Fundación Bariloche. Buenos Aires.

<sup>&</sup>lt;sup>2</sup> 1976. Geología del río Manso (Inédito). Fundación Bariloche, Departamento de Recursos Naturales y Energía. San Carlos de Bariloche.

## TRONADOR III UNIT

This unit, which forms the major part of the TVC (Figs. 2 and 3), overlies Tronador II and includes a diversity of lithologies and lithofacies. Two stratigraphic sections occur in this unit, defining two diachronic sequences referred to as the Meiling and Refugio Viejo stratigraphies (Fig. 4). The Meiling sequence (≈600-800 m in thickness; Fig. 2) is formed by meter to decimeter thick basaltic, basaltic andesite and andesite lava flows, hyaloclastic breccias, hyalotuffs, accretionary lapilli, lahars and proximal pyroclastic flows, suggesting magma-water interaction (Sheridan and Wohletz, 1983) for most of the lithologies forming this sequence. The Refugio Viejo sequence (>800 m thick) is formed by a sequence of meter thick andesitic lava flows, with

parallel stratification jointing, and basalts, both interbedded with hyaloclastic breccias, hyalotuffs, pyroclastic flows and laharic deposits (Fig. 4). Hyaloclastic breccias and lava flows of this subunit fill old glacial valleys. Lithologies and lithofacies forming both sequences suggest eruption under glacial conditions.

## **FONCK VOLCANO**

A well preserved pyroclastic cone, the source of a single andesite lava flow partially covering the Steffen unit of the SVC, is located to the south of the TVC (Fig. 1). The cone and lava flow shows no evidence of glacial erosion and are clearly younger than the last glacial cycle and probably Holocene in age.

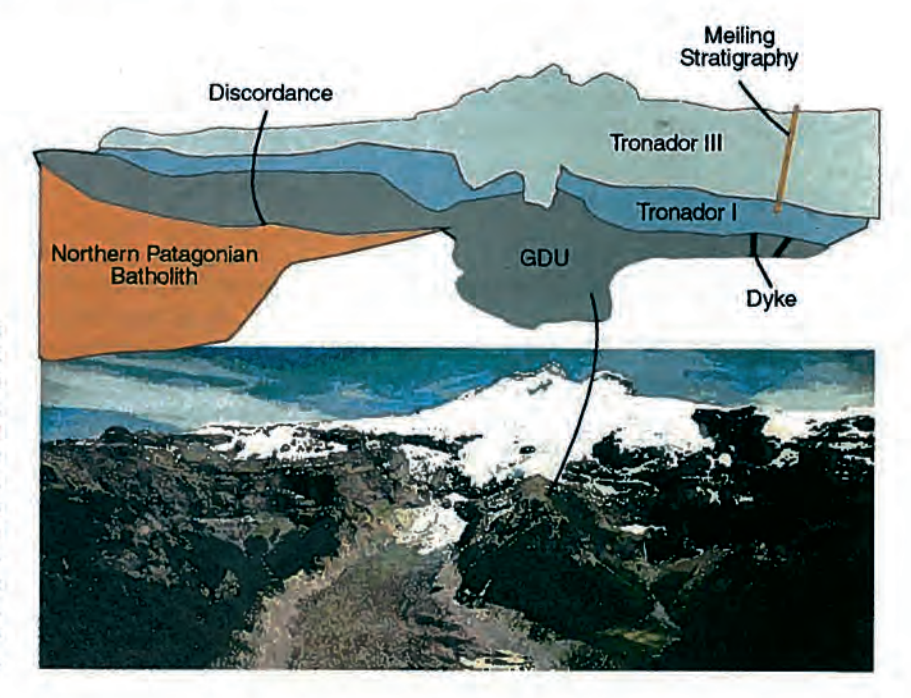


FIG. 2. View to the east of the Ventisquero Negro (center) and Garganta del Diablo valley (right), showing Tronador III overTronadorIunit, and dacitic necks, lavas and dykes of the Garganta del Diablo unit. Location of the Meiling stratigraphic section is also indicated (see Fig. 4). Photograph is courtesy of Sebastián de la Cruz.

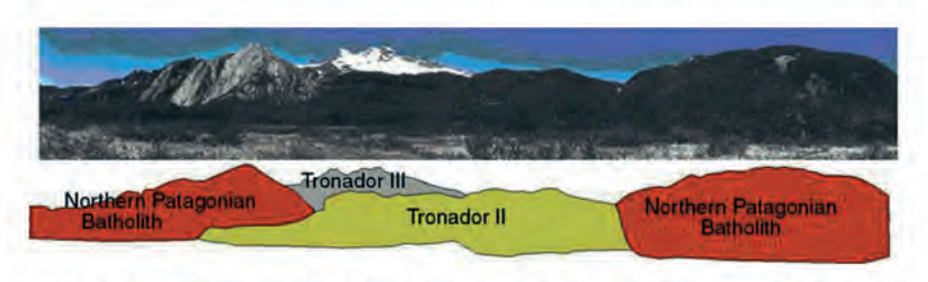


FIG. 3. View to the east of the La Veranada stratigraphic section through the Tronador II unit, which fills a glacial valley in granitic basement, and the overlying Tronador III unit in the background.

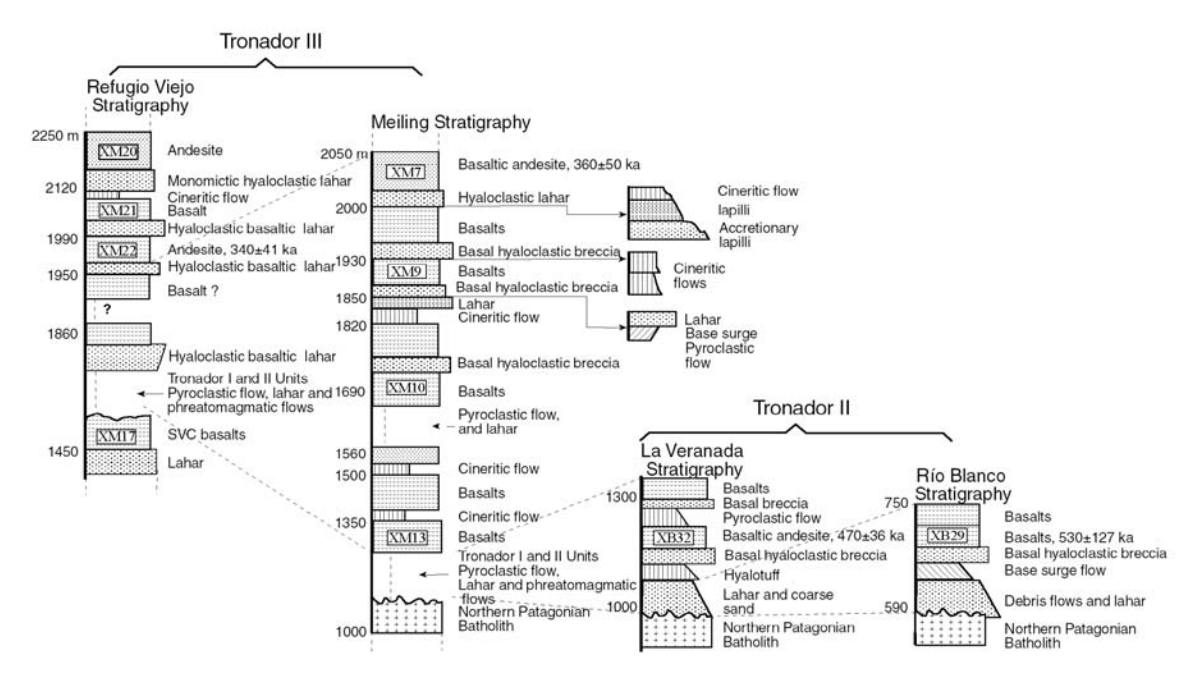


FIG. 4. Stratigraphic profiles for Tronador II (La Veranada and Río Blanco) and III (Meiling and Refugio Viejo) units, showing inter-bedding of lava flows and volcaniclastic facies related to magma-water interaction.

#### K-Ar AND Ar/Ar GEOCHRONOLOGY

Six samples from the TVG were selected for age determinations in the SERNAGEOMIN-Chile laboratory (Table 1), two for K-Ar and four for Ar/Ar, following the analytical procedures described by Duhart *et al.* (2001).

A whole-rock K-Ar age determination for a dacite lava from the GDU gave 1.3 ± 0.3 Ma, which is in agreement with ages of 1.32 and 1.39 Ma reported by Rabassa and Evenson (1986) for a 'volcanic rock interbedded with glacial deposits at the base of Cerro Tronador'. One K-Ar age reported by SERNAGEOMIN-BGRM (1985), probably collected at the base of the SVC (but reported as at the base of the Cuernos del Diablo volcano by Lara et al., 2001) eroded volcano, gave 0.7±0.4 Ma. These ages suggest that the volcanic activity forming both the GDU and probably the SVC started during the Early Pleistocene and not during the Pliocene. These ages are concordant with the age of the Pichileufú Drift reported by Rabassa and Evenson (1986); Rabassa et al. (1987) and Rabassa and Claperton (1990). Accordingly, based on field observations, stratigraphic relationships, degree of erosion and the geochronologic data (Table 1), the SVC and GDU would have approximately a similar

age and would be older than the TVC.

One whole-rock K-Ar determination for a lava flow from the Tronador I unit gave an age younger than 1.0 Ma (Table 1), below the detection limit of the equipment, confirming that this unit is younger than the GDU. Four total fusion Ar/Ar ages for Tronador II and III units gave Middle Pleistocene ages (Table 1, Fig. 4). The ages determined for samples from Tronador II are older (0.53±0.13 and 0.47±0.04 Ma) than the ages for samples from Tronador III (0.36±0.05 and 0.34±0.04 Ma).

These geochronological data suggest that volcanic activity in TVC started after 1.0 Ma and ended before the last two glacial cycles recognized in this region of the Andes, which occurred between approximately 262-132 and 70-14 Ka (Clapperton, 1993). Field observations document the existence of a thick volcanic sequence (400 m) between the Tronador II and III units, formed by consolidated phreatomagmatic deposits (tuffs and hyalotuffs), thin lava flows (<1.0 m in thickness) with rapid cooling textures, and hyaloclastites, all with different degrees of palagonitization. This sequence represents a complex succession of explosive and non-explosive hydrovolcanic activity in a subglacial

TABLE 1. Ar/Ar AND K-Ar AGES FOR SAMPLES FROM GDU AND TRONADOR I, II AND III UNITS.

## Ar/Ar, total fusion

Sample	Whole rock	Ca/K	CI/K	<sup>36</sup> Ar/ <sup>39</sup> Ar (Ca/Tot)	%³6Ar	<sup>40*</sup> Ar/ <sup>39</sup> Ar	<sup>39</sup> Ar	% <sup>40*</sup> Ar	Age (ka)	± erroi (2σ)
XB-29, Tron	ador II			,					•	` '
*10490-01	4	8.84369	0.04793	0.034132	4.4	0.21295	0.2018	2.2	429	124
*10490-02	4	8.5963	0.05291	0.03609	4.1	3.25215	0.1554	2.4	508	190
*10490-03	4	9.40146	0.04774	0.026444	6	0.28057	0.1748	3.7	566	68
Mean									530	127
XB-32, Tron	ador II									
•10487-01	4	2.86348	0.04615	0.003623	13.4	0.24156	0.1111	20.7	503	52
•10487-02	4	2.80011	0.05381	0.004594	10.4	0.22332	0.2373	15.5	465	30
•10487-03	4	2.34576	0.05462	0.002655	15	0.22571	0.1894	25.3	470	26
Mean									470	36
XM-7, Trona	idor III									
•10488-01	4	2.21706	0.07267	0.009386	4	0.13418	0.3497	4.8	270	65
•10488-02	4	2.07199	0.07307	0.026581	1.3	0.21709	0.4473	2.7	437	55
•10488-03	4	2.00648	0.0757	0.007461	4.6	0.17607	0.6894	7.7	354	27
Mean									360	50
XM-22, Tron	ador III									
•10489-01	4	1.84343	0.0664	0.016877	1.9	0.16375	0.5888	3.2	327	51
•10489-02	4	1.83110	0.0696	0.011733	2.7	0.16673	0.5363	4.7	333	28
•10489-03	4	1.89329	0.06773	0.019671	1.6	0.1827	0.4478	3.1	364	44
Mean									340	41

Sample XM	/I-23, GDUSamp	le XM-01.	Tronador I						
%K	Ar. Rad	%Ar	Age (Ma)	± error (2 σ)	%K	Ar. Rad	%Ar	Age (Ma)	± error (2σ)
1.85	0.11	91	1.5	0.4	0.582	0.013	98	< 1.0	-
1.85	0.081	96	1.1	0.5	0.582	0.011	98	-	-
					0.582	0.007	10	-	-
Mean				1.3	0.3				

environment (Mella *et al.*, 2003a, b). The magmaice interaction reflected in this sequence formed between 0.47 and 0.34 Ma ago, during a glacial cycle in part coinciding with that previous to the last two glacial cycles recognized at this latitude (Mercer, 1976; Porter, 1981) and with El Cóndor Drift of Rabassa *et al.* (1987) and Rabassa and Clapperton (1990).

The ages for Tronador III unit are older than all known ages for active volcanoes along the current volcanic front and minor eruptive centers (MEC) located to the west (for example, Osorno, Calbuco and Puyehue volcanoes; Thiele et al., 1985; Moreno et al., 1985; H. Moreno and B. Singer, personal communication, 2003). Thus, with the exception of the Fonck monogenetic cone, the volcanic activity forming the TVG is older than the activity along the present day volcanic front. Available K-Ar ages for

volcanic units west of the TVG include an Early Pleistocene K-Ar age (1.43±0.2 Ma), which is similar to the age of the volcanic activity that formed the GDU and the SVC, reported for the deeply eroded Hueñuhueñu volcanic sequence (H. Moreno, J. Varela, L. López-Escobar, F. Munizaga and A. Lahsen<sup>3</sup>; Thiele et al., 1985), and Early to Middle Pleistocene Chapuco Strata (1.0 to 0.4 Ma; SERNAGEOMIN-BGRM, 1995; Lara et al., 2001). Middle Pleistocene ages of 0.52±0.10 and 0.27±0.07 Ma were determined for La Picada eroded volcano and Reloncaví Strata, respectively (H. Moreno, J. Varela, L. López-Escobar, F. Munizaga and A. Lahsen<sup>3</sup>; R. Thiele, E. Godov, F. Hervé, M.A. Parada and J. Varela4). The ages of these volcanic units, located to the west of the TVG, suggest a wide arc during the Early-Middle Pleistocene evolution of the TVG compared to the current arc at this latitude.

<sup>3 1985.</sup> Geología y riesgo volcánico del volcán Osorno y centros eruptivos menores, Proyecto Hidroeléctrico Petrohué. Informe OICB-06C (Inédito), Empresa Nacional de Electricidad S.A.-Departamento de Geología de la Universidad de Chile, 212 p. Santiago.

<sup>4 1985.</sup> Estudio geológico-estructural regional y tectónico del área de Petrohué-Canutillar (Inédito), Empresa Nacional de Electricidad-Departamento de Geología de la Universidad de Chile, OICB-06C, 157 p. Santiago.

## **PETROGRAPHY**

Most of the petrographic information is based on lava flows samples representatives of the TVC and SVC (Fig. 4). Out of eighteen samples studied, thirteen belong to the TVC, three to the SVC, one to the GDU and one to the Fonck monogenic cone (Table 2). Samples from the SVC were collected in the northern part of this complex. Samples from Tronador II and III units were collected from outcrops on the southeast and southwest slopes of the TVC. Most of the Tronador I unit is covered by younger flows and is also difficult to access, limiting a representative sampling of this unit. Mineralogical compositions of selected samples were determined using the electron-microprobe equipment available at the Department of Geology of the University of Chile.

## **BASALTS**

Basalts occur mainly in the Tronador II and III units of the TVC and in minor proportion in the SVC. Basalts in the TVC are generally porphyritic (>30% phenocryst content), but cumuloporhyritic and aphanitic members are also present. Plagioclase is the predominant phenocryst (10-15 modal %, An<sub>90</sub>-An<sub>56</sub>), followed by olivine (Fo<sub>74</sub>-Fo<sub>54</sub>) and minor proportion of clinopyroxene (En<sub>38-45</sub>Fs<sub>19-21</sub>Wo<sub>38-41</sub>). Groundmass textures are mainly intergranular, intersertal or subophitic, formed by plagioclase microlites, olivine and clinopyroxene microcrysts, and volcanic glass.

Two different phenocryst associations have been recognized in the TVC: plagioclase-olivineclinopyroxene and plagioclase-olivine with orthopyroxene rims. The first one includes up to 80-90% euhedral zoned plagioclase phenocrysts (An<sub>e4</sub>-An<sub>e7</sub>) and subordinate olivine (Fo<sub>71</sub>) and clinopyroxene  $(En_{38-43}Fs_{19-20}Wo_{38-4}$ ; Fig. 5a). The groundmass is hyalopilitic and hyalophitic, with intergranular olivine microcrysts and subophitic clinopyroxene. This assemblage is observed both in the Tronador II and Tronador III units. Some lavas contain plagioclase crystals with sieve texture and resorbed edges while others show weak normal zoning (An<sub>64</sub>-An<sub>57</sub>, XB29). The second phenocryst association, which occurs mainly in the Tronador III unit and only in minor proportion in the Tronador II unit, includes strongly zoned euhedral plagioclase (Anon→Anes,

XM13) and olivine (Fo<sub>75</sub>→Fo<sub>58</sub>, Fig. 5b), in some cases with orthopyroxene rims. The Tronador III unit locally contains olivine basalts in which olivine has planar crystal edges, but in others olivine phenocrysts have embayed edges and plagioclase phenocrysts sieve textures (XM10, Table 1). Some basalts from Tronador III unit also include plagioclase xenocrysts with sieve textures and resorbed edges (XM21, Fig. 5c).

Basalts from the SVC contain olivine and clinopyroxene phenocrysts within a groundmass composed of plagioclase microlites, subophitic clinopyroxene and intersertal glass.

## **BASALTIC ANDESITES AND ANDESITES**

Porphyritic basaltic andesite is the dominant lithology in the SVC, with plagioclase and olivine phenocrysts, intergranular clinopyroxene and olivine, and intersertal glass. Basaltic andesites and andesites are mainly represented in the Tronador III unit of the TVC. They are porphyritic to cumuloporphyritic or aphanitic in texture, with small size phenocrysts (0.4-1.0 mm). Their groundmass is hyalopilitic and hyalophitic, composed of plagioclase microlites, intergranular iron oxides and intersertal tachilitic or sideromelane type glass.

Basaltic andesites from the TVC, as well as andesites from Fonck monogenic volcano, are formed by plagioclase, olivine and clinopyroxene phenocrysts. Andesites from Tronador III unit are composed of plagioclase, orthopyroxene and clinopyroxene, usually as cumulates (Fig. 5d). Trachytic and hyalopilitic textures with plagioclase microlites and glass are predominant in both the basaltic andesites and andesites.

## DACITES

Dacite is the dominant rock type in the GDU. Rock forming minerals include plagioclase, hornblende and orthopyroxene phenocrysts, with trachytic and hyalopilitic groundmass and iron oxides reaction rims around amphibole phenocrysts. This rock type is notable in a columnar jointed lava flow overlaying glacial deposits in the Garganta del Diablo Valley.

TABLE 2. PETROGRAPHY OF THE TVG, SHOWING COORDINATES, UNIT, TEXTURE, PHENOCRYSTS, GROUNDMASS, SECONDARY MINERALS AND LITHOLOGY OF THE SAMPLES.

XN-23         41111 18.03413         7119 28.03814         8118 28.03814         8118 28.03814         8118 28.03814         8118 28.03814         8118 28.03814         8118 28.03814         8118 28.03814         8118 28.03814         8118 28.03814         8118 28.03814         8118 28.03814         8118 28.03814         8118 28.03814         8118 28.03814         8118 28.03814         8118 28.03814         8118 28.03814         8118 28.03814 </th <th>Sample</th> <th>Latitude S</th> <th>Longitude W</th> <th>Unit</th> <th>Texture</th> <th>Phenocrysts</th> <th>Groundmass minerals</th> <th>Secondary</th> <th>Lithology</th>	Sample	Latitude S	Longitude W	Unit	Texture	Phenocrysts	Groundmass minerals	Secondary	Lithology
41*13*22.2823*         71*49*4.4046*         SVC         Aphlynic, trachylic         PI-OI         PI, integranular PACIFE         PI           41*13*22.2823*         71*52*58.2829*         SVC         Porphynitic, trachylic         PI-OI         PI, integranular Fe opaque mineral page and replaced page and repla	XM-23	41°11'18.0943"	71°50'2.9250"		Porphyritic and trachytic	PI-Hb-Opx	PI, intersertal and		Dacite
41*13*22.2823*         T1*55*8.2839*         SVC         Pophyritic tradhytic         PI-OI-Cpx         PI-Integranular Fe opeaque mineral integranular Fe opeaque mineral integranular Fe opeaque mineral integranular P-OI-ch integranula	XV-1	41°15'45.3846"	71°49' 44.4045"	SVC	Aphyric, trachytic	IO-IA	Infanchiniu grass PI, intergranular Px-OI- Fe opagija mineral		Basaltic andesite
41*117.1789;         71*62.56.2282*         SVC         Porphyritic         PHOID         PI, intergranular Px-OI, intersertal glass.         Pal           11 41*12.36.0313*         71*49.55.5328*         Tronador II         Porphyritic         PH-OI-Cpx         PI, intergranular Px-OI, intersertal glass.         Pal           41*117.5189         71*54.43.6383*         Tronador II         Aphyric, hyaloplilitic         PI-OI-Cpx         PI, intergranular Px-OI, intergranular Pal         Pal-Bow           41*10.58.8411*         71*54.43.6383*         Tronador II         Aphyric, hyaloplilitic         PI-Opx-Cpx         PI, intergranular Pal-Bow         Pal-Bow           41*10.58.8411*         71*57.43864*         Tronador III         Porphyritic, trachytic, PI-Opx-Cpx         PI, intergranular Pal-Boy         Pal-Bow           41*10.22.3300*         71*48.56.4897*         Tronador III         Porphyritic         PI-OI         PI, intergranular Pal-Boy         PI           41*10.22.3306*         71*48.38.0127*         Tronador III         Porphyritic         PI-OI         PI, intergranular Pal-Boy         PI           41*11.20.9568*         71*48.38.027*         Tronador III         Porphyritic, trachytic, PI-OI         PI, intergranular Ge opaque mineral         PI           41*11.20.9568*         71*22.3657*         Tronador III         Porphyritic, tr	XB-18	41°13'22.2823"	71°55'58.2599"	SVC	Porphyritic, trachytic	PI-OI-Cpx	Opaquo minoral PI, intergranular Fe opaque mineral intergranular Cox		Basaltic andesite
1	XM-17 XM-1	41°13'26.7457" 41°11'17.1789"	71°52′55.2262″ 71°49′55.3318″	SVC Tronador I	Porphyritic Porphyritic	PI-OI PIg-OI-Cpx	PI, intergranular Px-OI, intersertal glass PI, intergranular Cpx-OI and Fe	Pal	Basalt
41*17 55.5522*         72*0*41.6228*         Tronador II         Aphyric, hyaloplitic         PI-OpxCpx         PI-intersertal glass, subophitic Px and opeque mineral.         Pa-Bow opeque mineral           41*10*58.8411*         71*58*41.3854*         Tronador II         Porphyritic, trachytic, pa-Opphyritic, trachytic, pa-Opphyritic, trachytic, pa-Opphyritic, pa-O	XB-22-1		71°54' 43.6363"	Tronador II	Porphyritic	PI-OI-Cpx	opaque mineral PI, intersertal glass, intergranular	Pal	Basaltic andesite
41*10'58.8411"   71*58'41.3654"   Tronador II   Porphyritic, trachylic, pl-Opx-Cpx   Pl, intergranular Ol-Fe opaque mineral, subophitic Px and intersertal glass intergranular Ol-Fe opaque mineral subophitic Px and intersertal glass.   Tronador III   Aphyric   Pl-Ol-Cpx   Pl, intersertal glass, subophitic Px and intersertal glass, subophitic Px   Pl-Ol-Cpx   Pl-Ol-Cpx   Pl, intergranular Ol and Fe opaque mineral   Intergranular Ol and intersertal glass   Bow   Intergranular Ol and intersertal glass   Intergranular Ol and intersertal glass   Intergranular Ol	XB-29	41°13′55.5522″	72°0' 41.6228"	Tronador II	Aphyric, hyalopilitic	ā	Ol-Px, Fe opaque mineral Pl, intersertal glass, subophitic		Basalt
41*10*28.8411*         71*58*41.3654*         Tronador II         Porphyritic, trachytic, properties         Pi-Opx-Cpx         Pi-Intersental glass           41*10*22.3300*         71*36*74.9864*         Tronador II         Porphyritic, trachytic, properties         PI-OF	;			:	:	(	Opaque mineral.	Pal-Bow	Basalt
1 41*14 4.1831"         71*57'4.9864"         Tronador III         Porphyritic, trachytic, processes and p	XB-32	41°10′58.8411″	71°58'41.3654"	Tronador II	Porphyritic	Pl-Opx-Cpx	PI, intergranular OI-Fe opaque mineral, subophitic Px and intersertal relacs		Racaltic andecite
41°10′22.3300"         71°48′55.4697"         Tronador III         Aphyric         PI, intersental and hyalophtitic glass, intergranular Fe opaque mineral           41°10′22.3300"         71°48′55.4697"         Tronador III         Porphyritic         PI-OI         PI, intersental and hyalophtitic Dpx, intergranular OI and Fe opaque mineral         Idd-Bow           41°10′26.0251"         71°47′32.6287"         Tronador III         Porphyritic         PI-OI         PI, intergranular OI and Fe opaque mineral         Idd-Bow           41°11′20.9569"         71°47′8.4363"         Tronador III         Porphyritic         PI-OI         PI, intergranular OI and intersental glass.         Bow           41°11′20.9569"         71°47′12.8256"         Tronador III         Aphyric, hyalopilitic         PI-OI         PI, intergranular OI and intersental glass.         Bow           41°11′20.9569"         71°52′23.1657"         Tronador III         Aphyric, trachytic, hyalopilitic         PI-OI-Cpx         PI, intergranular Fe opaque mineral         Bow           41°12′7.5611"         71°52′33.5036"         Tronador III         Aphiric, trachytic, PI-OI-Cpx         PI, intergranular Pi, intergranular Pi         PI, intergranular Pi           41°12′7.5614"         71°52′34.3387"         Tronador III         Aphiric, trachytic, PI-Cpx         PI, intergranular Pi         PI, intergranular Pi           41°12′7.53	XB-14-1		71°57'4.9864"	TronadorII	Porphyritic, trachytic,	PI-OI-Cpx	Intersertal, PI-OI, subophitic Px		Basaltic andesite
41°10′29.9061"         71°48′36.0127"         Tronador III         Porphyritic         PI-OI         PI, intergranular OI and Fe opaque mineral intersertal glass.         Id-Bow           41°11′20.9569"         71°47′32.6287"         Tronador III         Porphyritic         PI-OI         PI, intergranular OI and Fe opaque mineral intersertal glass.         Bow           41°11′20.9569"         71°47′32.826"         Tronador III         Aphyric, hyalopilitic         PI-OI-Cpx         PI, intergranular OI and Fe opaque mineral intersertal glass.         Bow           41°11′29.4952"         71°52′23.1657"         Tronador III         Aphyritic, trachytic, hyalopilitic         PI-OI-Cpx         PI, intergranular Cpx. OI and Fe opaque mineral intersertal glass.         Bow           41°12′7.5611"         71°52′23.1657"         Tronador III         Porphyritic, trachytic, pl-OI-Cpx         PI-OI-Cpx         PI, intergranular Cpx, intergranular OI, intersertal glass.         PI, intergranular Cpx, intergranular CP           41°12′7.5611"         71°52′34.3387"         Tronador III         Aphiric, trachytic, pl-OI-Cpx         PI, intergranular Pe opaque mineral intersertal glass.         PI, intergranular Pe opaque mineral intersertal glass.	XM-7	41°10′22.3300″	71°48'55.4697"	Tronador III	Aphyric	PI-Cpx-Opx	PI, intersertal and hyalophitic glass, intergranular Fe opaque mineral		Basaltic andesite
41°10′56.0251"         71°47′32.6287"         Tronador III         Porphyritic         PI-OI         PI, intergranular OI and intersertal glass.           41°11′20.9569"         71°47′8.4363"         Tronador III         Porphyritic         PI-OI         PI, intergranular OI and intersertal glass         Bow           41°11′29.4952"         71°52′23.1657"         Tronador III         Porphyritic, trachytic, palopilitic         PI-OI         PI, intergranular Cpx-OI and Fe opaque mineral, intersertal glass         Bow           41°11′29.4952"         71°52′23.1657"         Tronador III         Porphyritic, trachytic, palopilitic         PI-OI         PI, intergranular Cpx, intergranular OI, intersertal glass.         Bow           41°12′7.5611"         71°52′33.5036"         Tronador III         Aphiric, trachytic, palopilitic         PI-OI         PI, intergranular OI, intersertal glass.           41°12′7.5611"         71°52′34.3387"         Tronador III         Aphiric, trachytic, palopilitic         PI-OI         PI, intergranular OI, intersertal glass, intergranular Pelopaque mineral           41°12′7.5611"         71°52′34.3387"         Tronador III         Aphiric, trachytic, palopilitic         PI-Cpx         PI, intergranular Pelopaque mineral	6-MX	41°10′29.9061″	71°48' 36.0127"	TronadorIII	Porphyritic	PI-OI	PI, intersertal glass, subophitic Opx, intergranular OI and Fe opaque mineral	Idd-Bow	Basalt
intersertal glass.  4 41°11′20.9569" 71°47′8.4363" Tronador III Porphyritic PI-OI PI-OI-Cpx PI, intergranular OI and intersertal glass Bow PI, 11′20.9569" 71°47′12.8256" Tronador III Porphyritic, trachytic, PI-OI PI-OI PI, intergranular Cpx-OI and Fe opaque mineral, intersertal glass Bow PI, 11′29.4952" 71°52′23.1657" Tronador III Porphyritic, trachytic, PI-OI PI, subophitic Cpx, intergranular OI, intersertal glass.  4 41°11′29.4952" 71°52′23.1657" Tronador III Porphyritic, trachytic, PI-OI PI, subophitic Cpx, intergranular OI, intersertal glass.  5 41°12′7.5611" 71°52′34.3387" Tronador III Aphiric, trachytic, PI-OI PI-Cpx PI, intersertal glass.  6 41°12′7.5611" 71°52′34.3387" Tronador III Aphiric, trachytic, PI-Cpx PI-OI PI, intersertal glass, intergranular Fe opaque mineral hyalopilitic PI-Cpx PI-Cpx-OI PI, intergranular Px-Fe opaque mineral pi-cpx-OI PI, intergranular Px-Fe opaque mineral	XM-10	41°10′56.0251″	71°47' 32.6287"	Tronador III	Porphyritic	PI-OI	PI, intergranular OI and Fe opaque mineral,		Basalt
<ul> <li>4 1°14′ 9571" 71°47′ 12.8256" Tronador III Aphyric, hyalopilitic PI-Ol PI, intergranular Cpx-Ol and Fe opaque mineral, intersertal glass Bow and Hall Porphyritic, trachytic, PI-Ol-Cpx PI, intergranular Fe opaque mineral, intersertal glass and hyalofitic glass.</li> <li>1 41°12′ 7.5611" 71°52′ 33.5036" Tronador III Porphyritic, trachytic, PI-Ol PI-Ol PI, subophitic Cpx, intergranular Ol, intersertal glass.</li> <li>2 41°12′ 10.9446" 71°52′ 34.3387" Tronador III Aphiric, trachytic, PI-Cpx PI, intersertal glass, intergranular Fe opaque mineral hyalopilitic PI-Cpx PI, intergranular Printergranular Printergranu</li></ul>	XM-13	41°11'20.9569"	71°47' 8.4363"	Tronador III	Porphyritic	PI-OI-Cpx	intersertal glass. PI, intergranular Ol and intersertal glass	Bow	Basalt
<ul> <li>41°11′29.4952" 71°52′23.1657" Tronador III Porphyritic, trachytic, hyalopilitic hyalopilitic</li> <li>1 41°12′7.5611" 71°52′33.5036" Tronador III Porphyritic, trachytic, PI-OI PI, subophitic Cpx, intergranular OI, intersertal glass.</li> <li>2 41°12′10.9446" 71°52′34.3387" Tronador III Aphiric, trachytic, PI-Cpx PI, intersertal glass, intergranular Fe opaque mineral hyalopilitic PI-Cpx-OI PI, intergranular PS-Fe opaque mineral opaque mineral hyalopilitic</li> <li>41°15′53.4815" 71°49′44.7543" Fonck Volcano Porphyritic PI-Cpx-OI PI, intergranular Px-Fe opaque mineral</li> </ul>	XM-14	41°14'.9571"	71°47' 12.8256"	TronadorIII	Aphyric, hyalopilitic	PI-OI	PI, intergranular Cpx-OI and Fe opaque mineral, intersertal glass	Bow	Basalt
41°12′7.5611" 71°52′33.5036" Tronador III Porphyritic PI-OI PI, subophitic Cpx, intergranular OI, intersertal glass.  2 41°12′10.9446" 71°52′34.3387" Tronador III Aphiric, trachytic, PI-Cpx PI, intersertal glass, intergranular Fe hyalopilitic pyaque mineral hyalopilitic PI-Cpx-OI PI, intergranular Px-Fe opaque mineral	XM-20	41°11' 29.4952"	71°52′23.1657″	TronadorIII	Porphyritic, trachytic,	PI-OI-Cpx	Pl, intergranular Fe opaque mineral, intersertal plass and hvalofitic plass		Andesite
2 41°12′10.9446" 71°52′34.3387" Tronador III Aphiric, trachytic, PI-Cpx PI, intersertal glass, intergranular Fe hyalopilitic PI-Cpx-Ol PI, intergranular Px-Fe  41°15′53.4815" 71°49′44.7543" Fonck Volcano Porphyritic PI-Cpx-Ol PI, intergranular Px-Fe opaque mineral	XM-21	41°12'7.5611"	71°52′33.5036″	Tronador III	Porphyritic	IO-IA	PI, subophitic Cpx, intergranular OI,		# # # # # # # # # # # # # # # # # # #
41°15'53.4815" 71°49'44.7543" Fonck Volcano Porphyritic PI-Cpx-Ol PI, intergranular Px-Fe opaque mineral	XM-22	41°12' 10.9446"	71°52′34.3387″	Tronador III	Aphiric, trachytic,	PI-Cpx	PI, intersertal glass, intergranular Fe		Andesite
	XV-2	41°15'53.4815"	71°49′44.7543″	Fonck Volcano		PI-Cpx-OI	PI, intergranular Px-Fe opaque mineral		Andesite

Cpx=Clinopyroxene; Opx=Orthopyroxene; OI = Olivine; PI = Plagioclase; Cpx = Clinopyroxene; Opx = Orthopyroxene; Fe opaque mineral = Magnetite, ilmenite. Idd = Iddingsite; Bow = Bowlingite; Pal=Palagonite. Aphyric=<10% Phenocrysts.

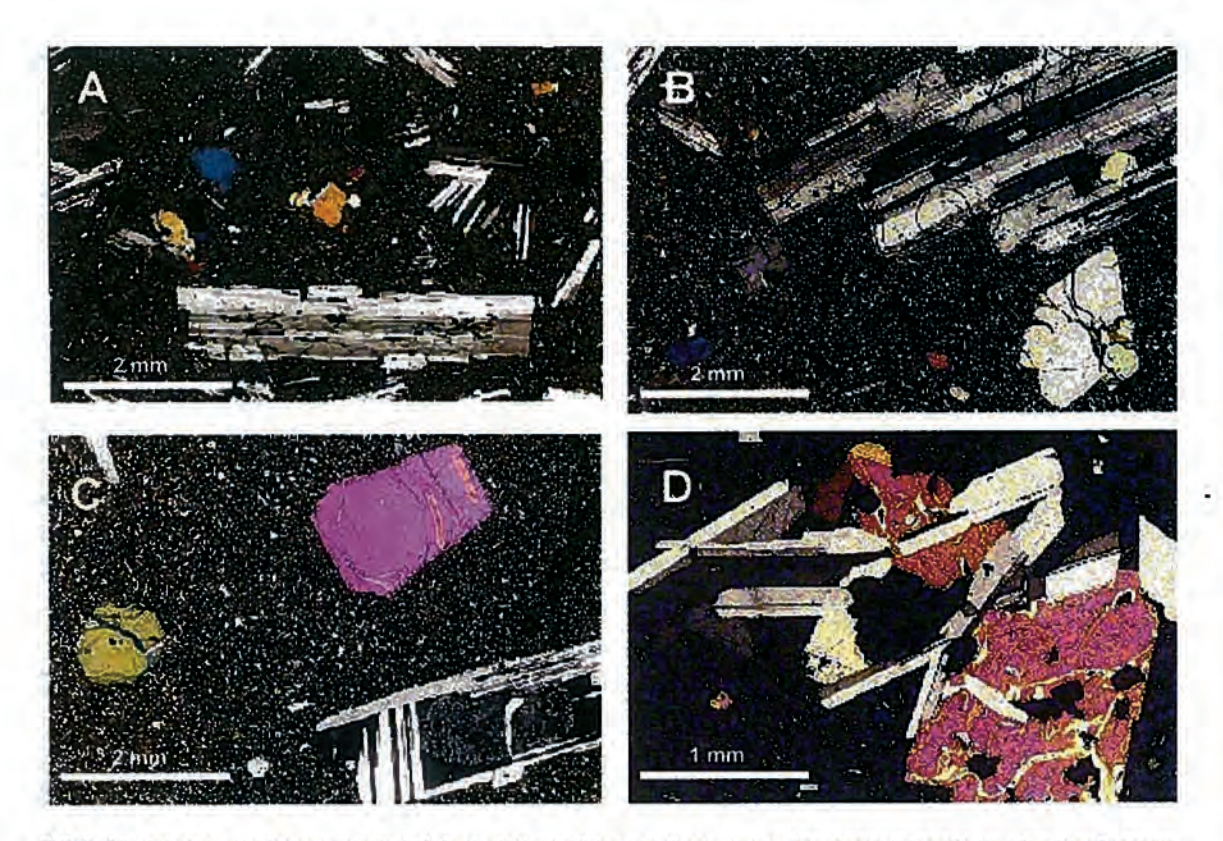


FIG. 5. Microphotographs (crossed nicoles) of: A- plagioclase, olivine and clinopyroxene phenocrysts in basaltic lava flow from Tronador III (sample XB22-1); B- plagioclase and olivine phenocrysts in basalt from Tronador III (sample XM9); C- olivine and plagioclase phenocrysts in basalt from Tronador III unit (sample XM21); D- plagioclase, clinopyroxene and orthopyroxene cumulate in andesite from Tronador III (sample XM7).

## PETROCHEMISTRY

## **METHODS**

Major and trace element chemical analyses of selected lava flows samples were determined at the chemical laboratory of SERNAGEOMIN-Chile (Table 3). Major elements were determined using atomic absorption spectrometry (AAS) and trace elements by a combination of Induced Coupled Plasma (ICP) with AAS (ICP-AAS) and optical emission (ICP-OES). Precision for trace elements is better than 10% and detection limit for Nb is 5 ppm.

## **MAJOR ELEMENTS**

Major element chemical compositions confirm the predominance of basalts, basaltic andesites and andesites in the TVC (Figs. 6 and 7). One sample from the Tronador I unit (XM1, Table 3) is basaltic andesitic in composition as are most of the lithologies forming this unit. Tronador II and III units also include both basalts and minor andesites. Basaltic andesites are more frequent than basalts in the SVC. The lava flow from Fonck monogenic cone is an andesite while samples from the GDU are essentially dacitic (Fig. 7).

Basalts are subalkaline in composition, none of them containing normative nepheline. Some basalts from the TVC are slightly undersaturated in SiO<sub>2</sub> as indicated by the absence of normative quartz and presence of normative olivine. In contrast, one basalt from the SVC is oversaturated in SiO<sub>2</sub> as indicated by normative quartz. Based on major (and trace) element chemistry, and following López-Escobar *et al.* (1995b), basic rocks (SiO<sub>2</sub><53 wt %)

TABLE 3. MAJOR, TRACE AND Sr and Nd ISOTOPIC COMPOSITION FOR SAMPLES FROM THE TVG.

	GDU	svc			Tronador I	Tronador II				Tronador
	XM23	XV1	XM17	XB18	XM1	XB29	XB22-1	XB14-1	XB32	XM7
Rock	dacite	bas. andes.	basalt	bas. andes.	bas. andes.	basalt	basalt	bas. andes.	bas. andes.	bas. ande:
Туре	medium-K	Group I	Group I	medium-K	Group I	Group II	Group II	high-K	Group II	high-K
_			_							_
SiO <sub>2</sub>	63.87	52.67	51.92	53.65	52.49	49.07	48.87	55.00	52.02	55.20
TiO <sub>2</sub>	0.63	1.00	1.23	1.43	1.02	1.97	1.68	1.95	2.03	1.85
$Al_2O_3$	16.85	17.48	19.17	17.16	18.04	15.87	17.37	15.48	16.50	15.65
Fe <sub>2</sub> O <sub>3</sub>	1.35	3.06	3.62	4.20	2.50	6.34	4.18	2.63	4.77	2.34
FeO	2.91	5.92	5.68	4.98	6.72	6.36	8.28	8.05	6.43	7.97
MnO	0.19	0.17	0.17	0.18	0.17	0.21	0.22	0.21	0.17	0.22
MgO	1.19	5.34	4.61	3.76	5.37	4.51	5.34	2.74	3.35	2.82
CaO	3.36	9.53	8.80	7.83	9.09	9.48	9.05	5.74	7.74	6.02
Na <sub>2</sub> O	5.32	3.10	3.30	3.61	3.10	2.77	3.21	3.71	3.53	3.91
$K_{2}O$	2.48	0.84	0.95	1.32	0.58	0.96	1.10	2.89	2.16	2.22
$P_2O_5$	0.25	0.19	0.19	0.27	0.17	0.36	0.36	0.50	0.38	0.54
LOI	1.20	0.55	0.35	1.30	0.70	1.99	0.28	1.07	0.85	1.02
Total	99.60	99.85	99.99	99.69	99.95	99.89	99.94	99.97	99.93	99.76
Rb	49	20	26	28	18	35.8	31	68	63	57.7
Ba	662	319	295	388	257	354	350	676	584	544
Sr	498	520	460	521	493	404	421	382	411	365
Zr	217	79	119	157	78	163	176	287	257	132
Nb	8	<5	<5	5	<5	6	5	9	9	8
Υ	28	17	17.2	20	17	33	31	30	44	48
Cr	159	107	108	100	166	67	45	116	47	75
Ni	34	26	28	21	37	37	45	12	18	11
Co	2	24	24	19	24	25	31	18	22	16
V	10	251	245	278	247	353	282	171	239	178
Sc	7	32	30	34	32	37	32	27	29	29
Cu	11	81	107	90	87	202	159	116	188	118
Zn	91	79	92	96	83	123	124	129	121	132
La	28.4	12.1	14.6	17.1	11.3	20	21	38	32	34
Ce	62.7	26.2	34	40.9	25	48	48	81	75	73
Pr	6.63	2.53	4	4.65	3	6.2	6.2	8.6	8.7	8.15
Nd	30	12.5	13.4	14.4	14.4	32.57	26	26	43.87	44.32
Sm	5.62	2.78	1.69	1.71	3.3	7.88	4.2	3.2	9.94	10.4
Eu	1.47	0.803	0.374	0.385	0.97	1	0.89	0.58	1.85	2.12
Gd	4.52	2.5	1.33	1.39	2.8	4.1	4	2.6	7.8	8.46
Tb	1.02	0.503	0.38	0.393	0.55	0.8	0.78	0.63	1.66	1.7
Dy	5.34	3.25	2.55	2.76	3.7	5.9	5.4	4.4	8.4	9.81
Но	1.2	0.719	0.602	0.7	0.88	1.25	1.19	1.09	1.8	2.2
Er	3.21	1.85	1.75	1.81	2.1	3.4	3.2	3.1	5.1	5.63
Tm	0.452	0.249	0.239	0.232	0.3	0.5	0.44	0.43	0.6	0.7
Yb	3.26	1.7	1.56	1.7	1.88	3.4	3.1	3.0	4.8	5.31
Lu	0.478	0.278	0.222	0.261	0.31	0.45	0.41	0.41	0.7	0.804
Ba/La	23.31	26.36	20.21	22.69	22.74	17.70	16.67	17.79	18.25	16.00
La/Yb	8.71	7.12	9.36	10.06	6.01	5.88	6.77	12.67	6.67	6.40
Ba/Rb	13.51	15.95	11.35	13.86	14.28	9.89	11.29	9.94	9.27	9.43
Rb/La	28.40	12.10	14.60	17.10	11.30	20.00	21.00	38.00	32.00	34.00
La/Nb	3.55			3.42		3.33	4.20	4.22	3.56	4.25
Ba/Nb	82.75			77.60		59.00	70.00	75.11	64.89	68.00
Sm/Yb	1.72	1.64	1.08	1.01	1.76	2.32	1.35	1.07	2.07	1.96
87Sr/86Sr						0.704172	·		0.704107	0.704156
<sup>143</sup> Nd/ <sup>144</sup> Nd						0.512807			0.512813	0.512790
$\epsilon_{\rm Sr}$						-4.7			-5.6	-4.9
ε <sub>Nd</sub>						+3.3			+3.4	+3.0
Nd		l			l	1 . 5.5			. 5. 1	

		Tronador III								Vo. Fonck
XB14-1	XB32	XM7	XM9	XM10	XM14	XM13	XM20	XM21	XM22	XV2
s. andes.	bas. andes.	bas. andes.	basalt	basalt	basalt	basalt	andesite	basalt	andesite	andesite
high-K	Group II	high-K	Group I	Group I	Group I	Group I	high-K	Group II	high-K	high-K
55.00	52.02	55.20	50.41	49.89	51.46	49.41	60.95	49.87	56.66	60.74
1.95	2.03	1.85	1.37	1.23	1.08	1.10	1.52	1.88	1.93	1.47
15.48	16.50	15.65	18.69	18.60	18.27	19.14	14.39	17.30	14.94	14.24
2.63	4.77	2.34	4.42	2.86	2.67	2.37	2.50	2.83	1.67	2.34
8.05	6.43	7.97	5.98	7.37	6.49	7.69	6.05	8.53	8.35	6.46
0.21	0.17	0.22	0.18	0.18	0.17	0.18	0.18	0.21	0.22	0.18
2.74	3.35	2.82	4.92	5.62	6.69	6.10	1.49	4.36	2.34	1.56
5.74	7.74	6.02	9.04	8.92	8.95	9.18	4.34	9.38	5.98	4.41
3.71	3.53	3.91	3.15	3.04	3.21	3.06	3.98	3.15	3.84	3.93
2.89	2.16	2.22	0.83	0.80	0.51	0.66	3.61	1.22	2.70	3.59
0.50	0.38	0.54	0.25	0.21	0.21	0.20	0.46	0.34	0.63	0.54
1.07	0.85	1.02	0.65	1.00	0.94	0.66	0.24	0.71	0.42	0.20
99.97	99.93	99.76	99.89	99.72	100.65	99.75	99.71	99.78	99.68	99.66
68	63	57.7	23	21	12	17	105	33	80.5	103
676	584	544	276	242	202	224	795	369	684	803
382	411	365	475	460	548	462	287	451	331	497
287	257	132	106	93	84	85	143	191	144	182
9	9	8	<5	<5	<5	<5	11	6	10	11
30	44	48	22	22	17	21	50	30	54	48
116	47	75	52	51	153	74	118	99	128	126
12	18	11	37	45	52	58	26	57	36	32
18	22	16	24	28	25	29	12	42	14	11
171	239	178	272	253	231	245	65	350	127	64
27	29	29	32	31	28	30	21	37	28	21
116	188	118	118	112	74	102	102	338	158	95
129	121	132	98	94	79	93	118	189	131	115
38	32	34	14	11.6	10.2	10.7	41	21	38	42
81	75	73	31	25.9	24	25	93	50	90	93
8.6	8.7	8.15	4	2.83	3	3.1	11.1	6	11.1	10.9
26	43.87	44.32	19	14.8	14	14.5	47	27	55.16	41
3.2	9.94	10.4	3.8	3.58	2.6	3.8	9.4	5	12.44	6.3
0.58	1.85	2.12	1	0.998	0.74	1.12	1.2	0.98	2.1	1.08
2.6	7.8	8.46	3.7	3.36	2.5	3.7	8.6	4.4	10.1	5.5
0.63	1.66	1.7	0.72	0.598	0.51	0.7	1.81	1.12	1.69	1.28
4.4	8.4	9.81	4.5	4.06	3.1	3.8	9.1	5.9	10.3	8
1.09	1.8	2.2	1	0.876	0.7	0.84	2.1	1.3	2.2	1.78
3.1	5.1	5.63	2.7	2.47	1.84	2.2	5.7	3.4	6	5
0.43	0.6	0.7	0.36	0.351	0.26	0.32	0.69	0.44	0.78	0.64
3.0	4.8	5.31	2.5	2.29	1.69	2.2	5.3	3.3	6.1	4.7
0.41	0.7	0.804	0.35	0.357	0.25	0.35	0.78	0.49	0.84	0.68
17.79	18.25	16.00	19.71	20.86	19.80	20.93	19.39	17.57	18.00	19.12
12.67	6.67	6.40	5.60	5.07	6.04	4.86	7.74	6.36	6.23	8.94
9.94	9.27	9.43	12.00	11.52	16.83	13.18	7.57	11.18	8.50	7.80
38.00	32.00	34.00	14.00	11.60	10.20	10.70	41.00	21.00	38.00	42.00
4.22	3.56	4.25					3.73	3.50	3.80	3.82
75.11	64.89	68.00					72.27	61.50	68.40	73.00
1.07	2.07	1.96	1.52	1.56	1.54	1.73	1.77	1.52	2.04	1.34
	0.704107	0.704156							0.704145	0.704192
	0.512813	0.512790							0.512782	0.512772
	-5.6	-4.9							-5.0	-4.4
	+3.4	+3.0							+2.8	+2.6

from the TVG are divided into two groups: Group I (relatively depleted basalts and basaltic andesites;  $\rm K_2O{<}0.96$  wt %; Rb<26 and La<14.6 ppm) includes samples from the older SVC and TVC I unit, as well as the younger Tronador III unit, while Group II (relatively enriched basalts and basaltic andesites;  $\rm K_2O{>}0.96$  wt %; Rb>31 and La>20 ppm) only includes samples from the younger Tronador II and

III units (Table 3). Group II basic rocks exhibit relative enrichment in  $\rm K_2O$ ,  $\rm TiO_2$ ,  $\rm Fe_2O_3$  and  $\rm P_2O_5$ , and depletion in MgO and  $\rm Al_2O_3$  compared to Group I (Fig. 6). Group I has similar MgO,  $\rm TiO_2$  and  $\rm P_2O_5$  contents as Osorno and Calbuco (López-Escobar *et al.*, 1992, 1995a) and Puyehue (Gerlach *et al.*, 1988) volcanoes, all of which being located along the current volcanic front.

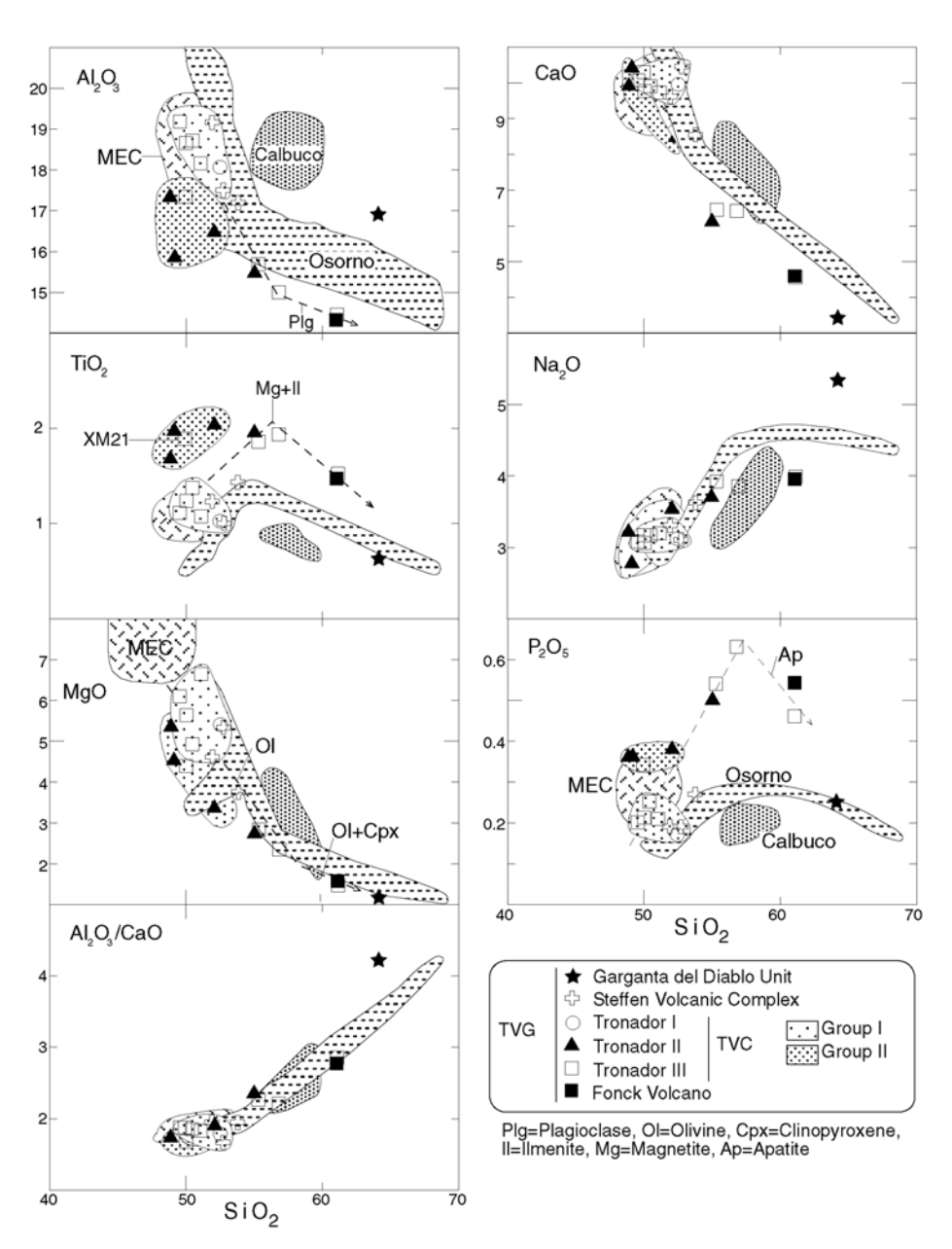


FIG. 6. Major elements and Al<sub>2</sub>O<sub>3</sub>/CaO versus SiO<sub>2</sub> diagrams for samples from the TVG. Data for Osorno, Calbuco and MEC are from López-Escobar et al. (1992, 1995a y b). Dashed lines represent compositional trends produced by crystallization of indicated minerals.

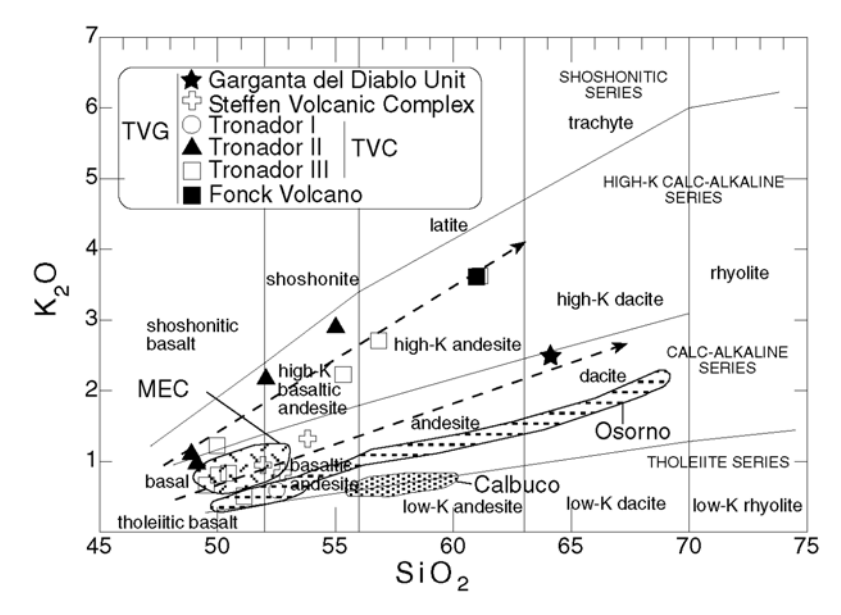


FIG. 7. SiO<sub>2</sub> versus K<sub>2</sub>O diagram for samples from the TVG. Data for Osorno, Calbuco and MEC are from López-Escobar et al. (1992, 1995a, 1995b). Tholeitic and calc-alkaline fields are from Peccerillo and Taylor (1976). Dashed lines represent differentiation trends of older GDU, SVC and Tronador I and younger Tronador II and III samples.

Tronador II and III exhibit increasing Na $_2$ O (2.77-3.21 wt %), Al $_2$ O $_3$ /CaO and decreasing MgO (3.4-6.69 wt %), CaO (7.7-9.5 wt %) and Al $_2$ O $_3$  (15.87-18.69 wt %) as SiO $_2$  increases (Fig. 6). Also, TiO $_2$  and P $_2$ O $_5$  increases in more basic samples of the Tronador III, but an inflection point is detected at intermediate compositions (SiO $_2$ =57 wt %) and these elements decrease at higher silica content. This is interpreted as Ca-plagioclase and olivine fractional crystallization in the basic members and Naplagioclase + iron oxides + orthopyroxene + apatite fractionation in the more differentiated ones.

Increasing Na $_2$ O (3.1-3.61 wt %), TiO $_2$  (1-1.4 wt %) and P $_2$ O $_5$  (0.19-0.27 wt %) related to decreasing CaO (9.53-7.83 wt %) and Al $_2$ O $_3$  (19.17-17.2 wt %) occur in basaltic andesites from the SVC and are related to Ca-plagioclase fractionation. For similar SiO $_2$  content, the TVC is depleted in MgO, Al $_2$ O $_3$  and enriched in K $_2$ O, TiO $_2$ , Fe $_2$ O $_3$  and P $_2$ O $_5$  compared to the SVC.

For more differentiated rocks, two different affinities are clear on the  $\rm K_2O\text{-}SiO_2$  diagram (Fig. 7). Differentiated rocks from the older GDU and the SVC are medium-K in composition, as are differentiated rocks from the current volcanic front, while differentiated rocks from the younger Tronador II and III units and the Fonck center are high-K in composition.

## TRACE ELEMENTS

## Ni, Cr, Sr, Sc and V

Ni and Cr, as well as MgO contents of all basalts analyzed from TVG are lower than those expected for magmas in equilibrium with peridotite mantle (MgO=11-15%, Ni =1500 ppm and Cr =2200; Frey et al., 1978), suggesting that fractional crystallization processes have occurred. As a consequence of fractional crystallization, the Sc (37-21 ppm), V (353-127) and Sr (548-287) contents decrease with increasing SiO<sub>2</sub> in samples from the TVC. In the Tronador III unit, Ni (58-11 ppm) decreases while Cr (84-143 ppm) increases with increasing SiO<sub>3</sub> indicating fractional crystallization involving more olivine than clinopyroxene. This tendency is less clear for Tronador II (Table 3). In the case of the SVC, on the other hand, both Ni and also Cr decrease with increasing SiO2, suggesting fractionation of both olivine and clinopyroxene.

## Ba, Rb, Zr, Nb and REE

Rb, Ba,  $K_2O$ , La, Zr and Nb increase with increasing  $SiO_2$  for all the samples from the TVG. Group I basic rocks from the TVG have Rb=12-26 ppm, Ba=202-319 ppm, La=10.2-14.6 ppm, Zr=84-

119 ppm and Nb<5 ppm (lower than the detection limit). Group II basalts from the Tronador II and III units have higher concentrations of these elements, Rb=31-63 ppm, Ba=354-584 ppm, La=20-32 ppm, Zr=163-295 ppm and Nb=5-9 ppm (Table 3, Fig. 8).

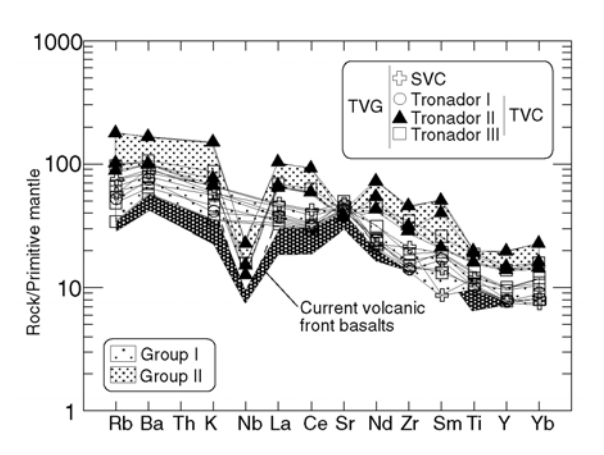


FIG. 8. Multi-element spider diagram for basalts from TVC Group I and II mafic rocks compared to those from the SVC and basalts from the current volcanic front (Hickey-Vargas et al., 1986; Gerlach et al., 1988). Normalizing values are from Sun and McDonough (1989).

REE pattern for all basic samples from the TVC are relatively flat, with La/Yb ratios in the 4.9-6.8 range. However, both REE contents and La/Yb ratios for all TVG samples are higher than those for the current volcanic front (Fig. 9). Group II (La/Yb=5.9-6.8) samples have slightly higher REE and La/Yb than Group I (4.9-6; Fig 9B). Similar trends in SVZ volcanic centers along the volcanic front compared to those from behind the front have been associated with higher degrees of partial melting below the front (López-Escobar et al., 1976, 1977; Hickey-Vargas et al., 1986, 1989; Stern et al., 1990; López-Escobar et al., 1993, 1995b). However, although Group I samples from the SVC have similar La than those from the TVC, they have lower Yb, and thus higher La/Yb, than Group I samples from the TVC (Fig. 9C). La/Yb ratios are relatively constant as SiO<sub>2</sub> increases (Fig. 9A), but Group II samples evidence a stronger negative Eu anomaly compared to Group I rocks (Fig. 9B).

Group I samples have higher Ba/La, Ba/Rb (Fig. 10) and Ba/Nb, and lower K/Rb ratios than Group II basic rocks (Table 3). Similar trends in volcanic centers from behind the Andean SVZ volcanic front,

compared to those along the front, have been associated with a greater input of fluids derived from the subducted plate below the front (López-Escobar *et al.*, 1976, 1977; Hickey-Vargas *et al.*, 1986, 1989; Stern *et al.*, 1990; López-Escobar *et al.*, 1993, 1995b).

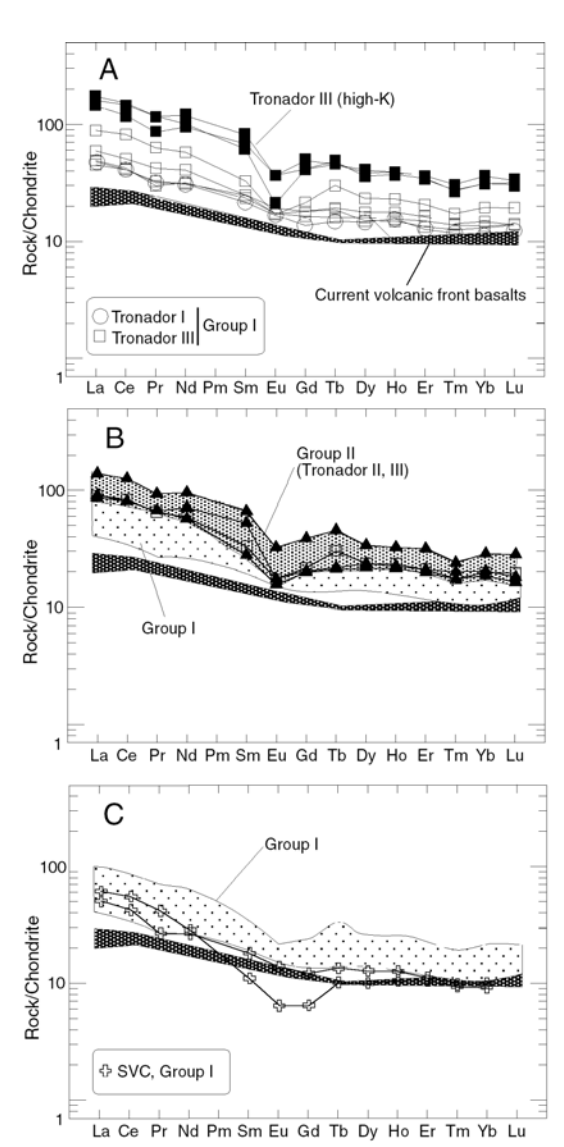


FIG. 9. A- REE abundances for basic (<53% SiO<sub>2</sub>) and intermediate (>56% SiO<sub>2</sub>) compositions from Tronador I and III units showing enrichment relative to the current volcanic front, **B-** REE abundances for samples from Tronador II (Group II) compared to Tronador I and III unit (Group I) and the current volcanic front; **C-** Group I samples from the SVC compared to the fields of Group I from the TVC and the current volcanic front. Chondrite values are from Sun and Mcdonough (1989). Field for the current volcanic front is represented by data from Hickey-Vargas *et al.* (1986) and Gerlach *et al.* (1988).

## Sr AND Nd ISOTOPES

Sr and Nd isotopic ratios were determined on Group II basalt and basaltic andesite from the Tronador II subunit, high-K basaltic andesite and andesite from Tronador III, and an andesite from the Fonck monogenic center (Table 3). Isotopic analyses were done at University of Colorado, Boulder, USA, by isotopic dilution mass spectrometry as described by Farmer *et al.* (1991).

Sr isotopic ratios range between 0.704107 and 0.704192 (Table 3). The lower value is presented by a basaltic andesite from Tronador II and the higher by the andesite from the Fonck monogenic center. Nd isotopic ratios are between 0.512773 and 0.512813, with the highest value belonging to the basic rocks from Tronador II and the lowest

value belonging to the Tronador III and Fonck andesites. In the <sup>87</sup>Sr/<sup>86</sup>Sr **versus** <sup>143</sup>Nd/<sup>144</sup>Nd diagram (Fig. 11), these rocks show a negative correlation, plot in the mantle array and have similar Sr and Nd isotopic ratios than other samples from the Andean CSVZ and SSVZ (37-46°S), but plot outside the field of samples from the NSVZ and TSVZ (33-37°S).

As for most volcanoes along the SVZ, the Sr isotopic ratios of rocks from the TVG are independent of their SiO<sub>2</sub> and Sr contents (Table 3). This is interpreted as a lack of significant amount of crustal assimilation in conjunction with fractional crystallization (Stern, 1988, 1989, 1991; Gerlach *et al.*, 1988; Hickey-Vargas *et al.*, 1989).

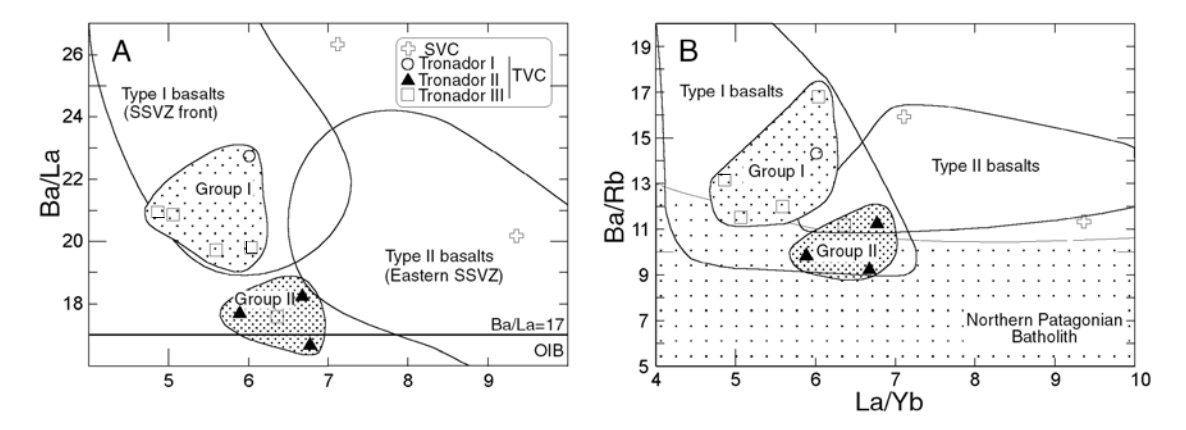


FIG. 10. **A-** Ba/La *versus* La/Yb and B. Ba/Rb *versus* La/Yb comparing samples from the TVC and SVC with fields for Type I and II basalts (López-Escobar *et al.*, 1993, 1995b) and in **B-** for granitoids nearby the TVG belonging to the Northern Patagonian Batholith (data *in* SERNAGEOMIN, 1998).

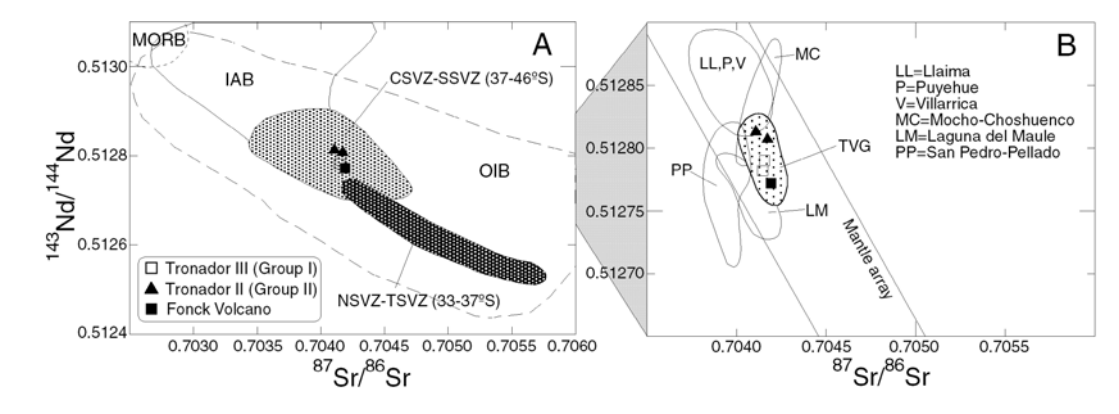


FIG. 11. **A-** <sup>143</sup>Nd/<sup>144</sup>Nd *versus* <sup>87</sup>Sr/<sup>86</sup>Sr diagram for samples from the TVG and fields for the SVZ between 37 and 41°S. **IAB**=island arc basalts; **OIB**=oceanic island basalts; **SVZ**=Southern Volcanic Zone at 37°-41°S and 33°-37°S and **MORB**=mid-oceanic ridge basalts. Modified from López-Escobar (1993); **B-** <sup>143</sup>Nd/<sup>144</sup>Nd *versus* <sup>87</sup>Sr/<sup>86</sup>Sr diagram for samples from the TVG compared with volcanoes along the current volcanic front (McMillan *et al.*, 1989).

## DISCUSSION

## **GENERAL**

Trace elements compositions of all samples from the TVG, specifically enrichment in LILE and depletion in HFSE relative to REE (Figs. 8 and 9), suggest that these rocks originated by partial melting of the asthenospheric mantle wedge contaminated with fluids from the subducted Nazca Plate. This is because Rb and Ba are mobile and Nb and Ti immobile compared to REE in high-pressure and high-temperature aqueous fluids such as those derived by the high-pressure dehydration of the subducted slab (Tatsumi and Eggins, 1995; Best and Christiansen, 2001). Samples from the TVG have high Ba/Rb (Fig. 10, Table 3) and K/Rb and low K/Ba, K/La, and Rb/La ratios compared to crustal rocks, indicating that the mainly granodioritic basement is not the cause of LILE enrichment relative to REE. This last has also been suggested for some other volcanic centers along the current SVZ volcanic front (for example, Mocho-Choshuenco, McMillan et al., 1989). This is especially clear for the Tronador III unit, in which K/Rb, Rb/La, Ba/La and La/Yb (Fig. 10, Table 3) ratios are similar for both basic and more differentiated samples. Morever, Sr isotopic ratios independent of SiO<sub>2</sub> and Sr contents preclude intracrustal contamination in the genesis of either basic or more differentiated rocks from the TVC, as discussed by Hickey-Vargas et al. (1986, 1989); Futa and Stern (1988) and Stern (1988).

All TVG basalts are enriched in  $\rm K_2O$ ,  $\rm TiO_2$ ,  $\rm Fe_2O_3$ ,  $\rm P_2O_5$ , Rb, Ba, Nb, Zr, and LREE compared to basalts erupted along the current volcanic front (Figs. 8 and 9), for which derivation by 10-12% partial melting of a mantle source is considered appropriate (López-Escobar *et al.*, 1976, 1977). The geochemical characteristics of TVG basalts are, therefore, interpreted as the result of somewhat lower degrees of partial melting than below the current front.

Two geochemical groups have been recognized for basic samples from the TVG, Group I (relatively depleted) and Group II (relatively enriched), similar to the division between Type I and Type II basalts proposed for other volcanic centers of the SVZ by López-Escobar *et al.* (1993, 1995b). However, López-Escobar *et al.* did not recognize these two types in a single stratovolcano. Type I basalts, with high Ba/La and low La/Yb ratios (Fig. 10) are

represented in volcanic centers located along the volcanic front to the west and Type II basalts, with lower Ba/La and higher La/Yb ratios, in centers located to the east of the front. These compositional changes, which are observed from west-to-east among the volcanic centers aligned along structures obliques to the LOFS (for example, Villarrica-Quetrupillán-Lanín; Hickey-Vargas et al., 1989), have been attributed to decreasing input to the east of components derived from the dehydration of the subducted slab (Hickey-Vargas et al., 1984, 1986; 1989; Stern et al., 1990; López-Escobar et al., 1992, 1995b). The coexistence of these two groups in the single TVC stratovolcano must, therefore, result from temporal variations of these same factors over a relatively short time period. Detailed models for basic and more differentiated rocks from the TVC are discussed below.

## **BASALT PETROGENESIS**

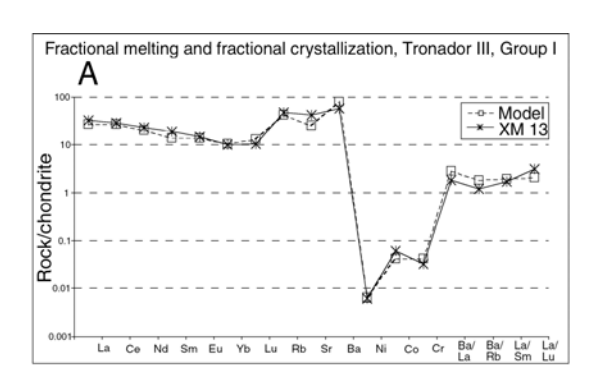
In order to explain the compositional changes in the TVG basalts, models were calculated for different degrees of bulk partial mantle melting and subsequent crystallization following the general conditions suggested by López-Escobar et al. (1976, 1977), which indicate derivation of Type I basalts along the current volcanic front by 10-12% bulk partial melting of garnet-free mantle peridotite. Partition coefficients were taken from those of basaltic lavas published by Rollinson (1993, p. 108-110), with values normalized to the chondritic abundances of Sun and McDonough (1989). Rare earth and other trace elements concentrations for peridotitic mantle were taken from Frey et al. (1978). Mantle mineralogy was that of Green and Ringwood (1967), with 50-60% olivine, 10-20% orthopyroxene, 10-25% clinopyroxene, and 3% garnet for the SVC, or 0% garnet for the TVC, and melting of 25% olivine, 25% orthopyroxene, 49% clinopyroxene, and 1% garnet for the SVC, or 0% garnet for the TVC.

For Group I samples from the older SVC and younger TVC, the degree of partial melting of the mantle was 10% and 7%, respectively, followed in both cases by 5-20% fractional crystallization of plagioclase, olivine and clinopyroxene (Fig. 12). The presence of garnet in the source of the SVC is indicated by their lower Yb contents and higher La/Yb ratios, and implies a deeper mantle source for

these older samples. Relative to these models, samples of Group I rocks from both the SVC and TVC are strongly depleted in Nb, slightly depleted in HFSE, and slightly enriched in Sr and Ba/La ratio (Fig. 12). This is consistent with the modification of the mantle source by the addition of slab derived components (López-Escobar *et al.*, 1976, 1977; Hickey-Vargas *et al.*, 1984, 1986, 1989).

Group II samples from Tronador II and III gave good correlation with 6% bulk partial melting of a garnet free asthenospheric mantle followed by 50-60% of fractional crystallization of 14% olivine, 7% clinopyroxene and 79% plagioclase (Fig. 13A). However, such a high percentage of fractional crystallization is not coherent with the basic composition of these samples. Compared with TVC

Group I, the composition of Group II samples (characterized by relatively high Nb, Ti and Yb contents, higher La/Nb and La/Yb and lower Ba/La ratios) suggest lower degrees of partial melting of a garnet-free mantle, with participation of less subduction components. An alternative model for Group II gave a satisfactory result with 5% partial melting of mantle with 5% of plagioclase (see Fig. 13B), followed by 20% fractional crystallization. At the latitude of the TVG the crust is only about 35 km thick (Lowrie and Hey, 1981) and plagioclase could be stable in the upper part of the lithospheric mantle, which due to the increase of temperature associated with arc volcanism could melt (Best and Christiansen, 2001).



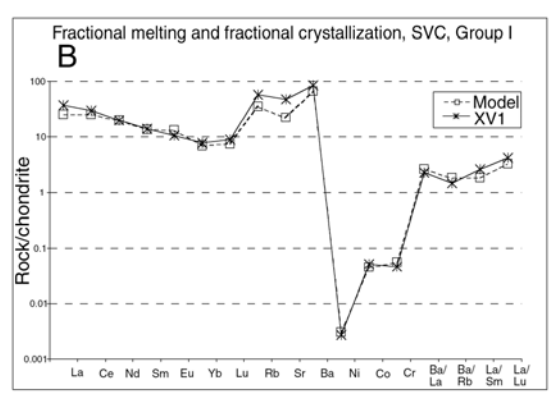
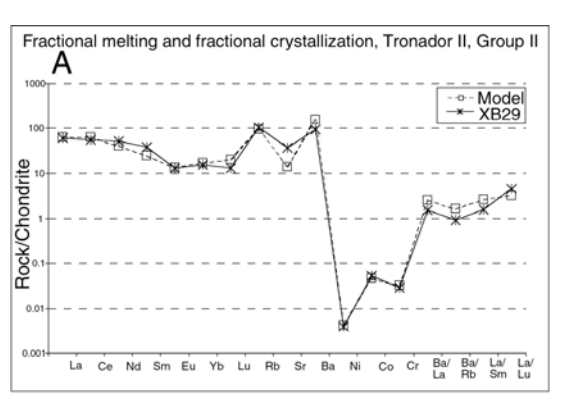


FIG. 12. **A-** Fractional partial melting and crystallization model for younger TVC Group I sample XM13 from the Tronador III unit. **B-** Fractional melting and crystallization model for older SVC Group I sample XV1. Models involve 7% and 10%, respectively, of bulk partial melting of peridotitic mantle formed by 50%-60% olivine, 17%-25% orthopyroxene, 19%-25% clinopyroxene and 0% garnet for the TVC and 3% garnet for the SVC sample; melting as follows of 25% OI, 24% Opx, 50% Cpx, 0-1% Gr for the SVC, with 5% of fractional crystallization of 60% Plg, 10% OI, 30% Cpx for the TVC and of 30% OI, 10% Cpx and 60% Plg for SVC.



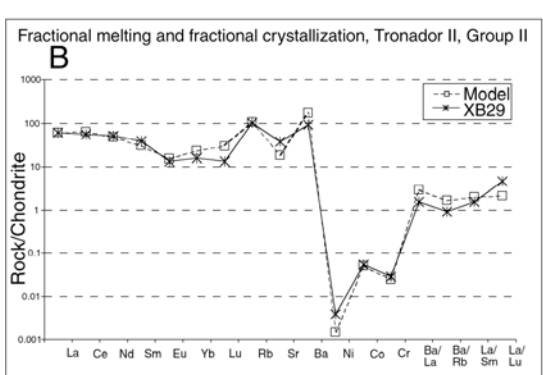


FIG. 13. Two different fractional partial melting and crystallization model for Group II sample XB29 from the Tronador II unit. A- Model involves 6% fractional partial melting of a garnet free mantle followed by 50-60% fractional crystallization of 14% OI, 7% Cpx and 79% PIg; B- Model involves 5% fractional partial melting of plagioclase bearing mantle followed by fractional crystallization of 20% OI, 20% Cpx and 60% PIg.

## **ANDESITE PETROGENESIS**

Major and trace element compositions of the basaltic andesites and andesites from the TVC suggest derivation from basaltic magmas by fractional crystallization. Basalts, basaltic andesites and andesites have parallel REE patterns (Fig. 9). In addition, Sr isotopic ratios suggest that crustal contamination was negligible.

The Sr and Ni compositions of basalts from the TVC are coherent with Ca-rich plagioclase and olivine crystallization. Cumulates of clinopyroxene and orthopyroxene were observed in andesites from Tronador III unit (XM7). Tronador III unit exhibits increasing Cr content with increasing SiO, composition suggesting that cumulates in the evolved lavas of this unit are related to fractionation of clinopyroxene and orthopyroxene. Models using REE, Ni, Cr, Co, Rb and Ba compositions and Ba/ La, Ba/Rb, La/Sm and La/Lu ratios shows that XM07 andesite can be produced by 60% fractional crystallization of 60% plagioclase and 40% olivine from basalt XM9 (Fig. 14A), confirming late fractionation of pyroxenes as suggested by initially increasing Cr as SiO<sub>2</sub> increases. Andesite XM20 can be produced by 60% fractional crystallization of 50% plagioclase, 20% olivine and 30% clinopyroxene from basalt XM13 (Fig. 14B).

# EVOLUTION OF THE QUATERNARY VOLCANIC ARC AT 41°10'S

The chronologic and petrochemical data for the TVG constrain the understanding of the evolution of the genesis and evolution of the Quaternary Andean volcanic arc at this latitude. Early Pleistocene SVC basic magmas formed by a relatively high degree of partial melting associated with the input into the mantle wedge of relatively large amount of fluids from the subducted slab. These conditions are similar to those that would have generated the late Middle Pleistocene-Holocene volcanism along the current volcanic front, but at somewhat greater depths (Fig. 15A). Middle Pleistocene rocks from the TVC (<1.0 Ma to 300 ka) have geochemical characteristics (high K<sub>2</sub>O, TiO<sub>2</sub>, Ba, Rb and HFSE) consistent with volcanism behind the volcanic front and were produced by lower degree of partial melting than below the current volcanic front (Fig. 15B). The observed temporal petrochemical

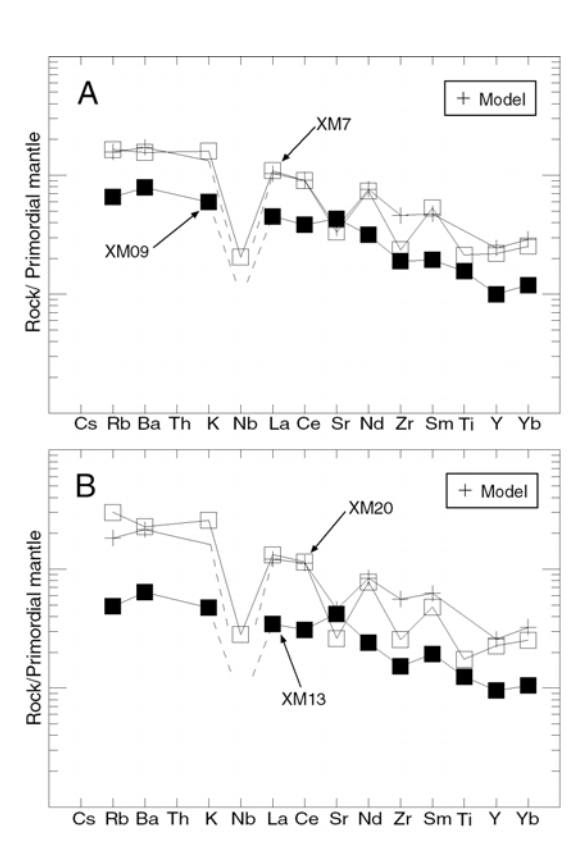
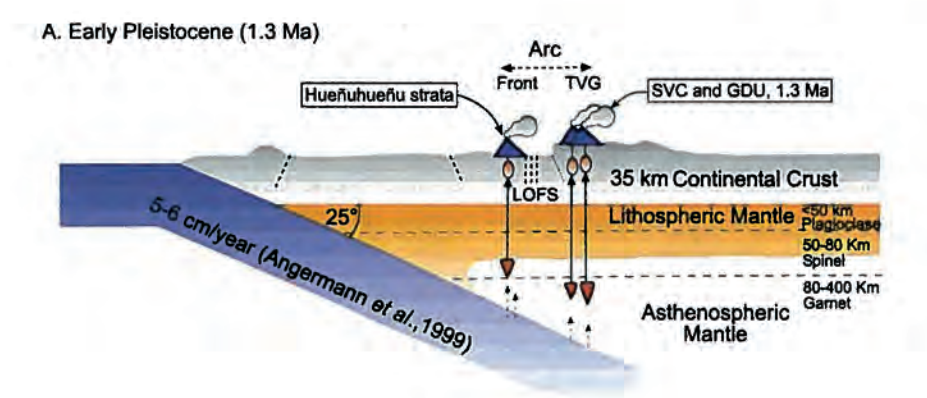


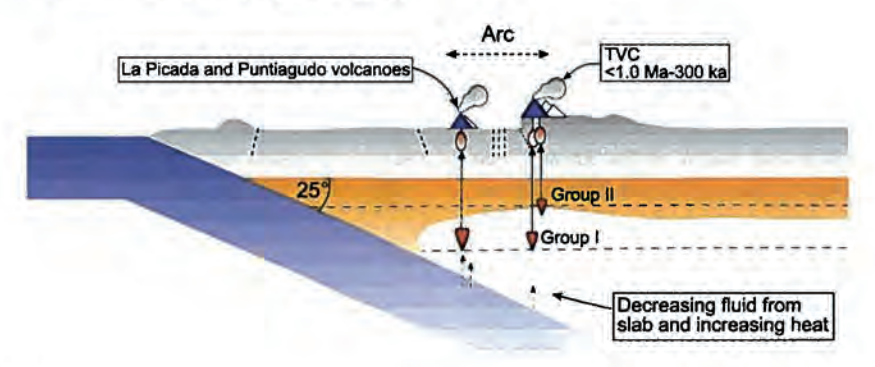
FIG. 14. Fractional crystallization model for TVC andesites. A-Andesite XM7 generated by 60% fractional crystallization of 60% Plg and 40% OI from basalt XM9. **B-** Andesite XM20 produced by 60% fractional crystallization of 50% Plg , 20% OI and 30% Cpx from basalt XM13.

changes, such as decreasing of the Ba/La ratios, suggest that these differences were associated with decreasing input of slab-derived fluids into the subarc mantle. These temporal variations are similar to the spatial variations occurring across volcanic lineament oblique to the volcanic front (for example, Villarrica-Quetrupillán-Lanín). Finally, the TVC volcanism ended during the late Middle Pleistocene when the stratovolcanoes forming the current volcanic front began to form, and subsequent TVG volcanic activity, which formed the Fonck monogenic center during the post-glacial-Holocene, was relatively minor (Fig. 15C).

Available Early to Middle Pleistocene ages for the eroded La Picada volcanic center and Hueñuhueñu and Chapuco volcanic strata (Moreno *et al.*, 1985; SERNAGEOMIN-BGRM, 1995; Lara *et al.*, 2001), located west of the TVG, suggest a wide arc



## B. Middle Pleistocene (<1.0 Ma-300 ka)



## C. Middle to Late Pleistocene-Holocene (300 ka - present)

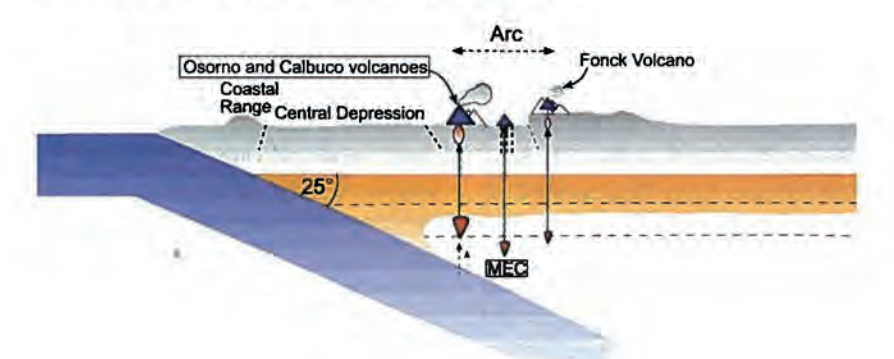


FIG. 15. Schematic cross section showing evolution for the TVG as part of the Andean Quaternary volcanic arc at 41°S since Early Pleistocene to the present day. A- Possible configuration during the Early Pleistocene (1.3 Ma) producing the SVC and GDU with Ba/La similar to the current volcanic front, indicating high fluid input from the subducted slab causing 10% melting of the garnet-bearing asthenosphere. B- Possible configuration during the Middle Pleistocene (<1.0 Ma to 300 ka) with decrease influx of subducted components and consequently lower percent of partial mantle melting producing Group I and Group II in the TVC; C-configuration during the Middle to Late Pleistocene-Holocene showing ending of activity at the TVC, presence of minor volcanism at the post-glacial Fonck monogenic cone and generation of the current volcanic front. Plate configuration and crustal thickness are from Bevis and Isacks (1984) and Lowrie and Hey (1981). Stability for garnet, spinel and plagioclase are from Köhler and Brey (1990). MEC: Minor Eruptive Centers.

at this latitude during the Early to Middle Pleistocene evolution of the TVG compared with the current arc. At this latitude, the active stratovolcanoes of the current volcanic front began to form only after the activity in the TVC ended. Several hypotheses have been proposed to explain similar changes in the configuration and/or in the amplitude of the Quaternary volcanic arc in the segment of the SVZ to the north of the TVG, including continental accretion, a possible increase in the subduction angle, and heating of the mantle wedge due to changes in the vigor of asthenospheric mantle convection associated, possibly, with changes in the convergence velocity (Stern, 1989; Lara et al., 2001). Since it appears that only the amplitude and not the location of the volcanic front may have occurred at this latitude, it is unlikely that the geometric configuration of the subducted Nazca plate has changed during the Pleistocene. However, the petrochemical models for the evolution of the TVG suggest progressive shallowing of the zone of melting, which might indicate asthenospheric heating as the cause of the westward migration of the main locus of volcanism to below the current volcanic fronts. For the SVZ arc segment between 38°-39°S, Stern (1989) also proposed an increase in the heat input from the convecting asthenospheric mantle. Below the TVG, heating also apparently occurred in conjunction with a decrease in the input of slab-derived fluids into the mantle wedge, which caused the percent of mantle partial melting below the TVG to decrease at the same time that the zone of melting shallows.

The change in the petrochemistry of TVG magmas ascribed to a combination of a decrease in fluid input from the subducted slab and shallowing of the mantle source caused by heating in the wedge occurred gradually between the Early and Middle Pleistocene, and may have resulted from a reduction in the convergence rates from 9 cm/yr to 7.9 cm/yr (Engebretson et al., 1986) or 5-6 cm/yr (Angermann et al., 1999) that occurred at approximately 2.0 Ma, as proposed by Lara et al. (2001). However, in contrast, the change in the amplitude of volcanic activity across the volcanic arc, and the formation of the active volcanoes along the current front to the west of the TVG, occurred rather relatively abruptly during the Late Middle Pleistocene after 300 ka, almost 2 Ma after the velocity of convergence decreased.

## **ACKNOWLEDGEMENTS**

The authors thank A. Schilmer, owner of Hostería Peulla, and A. Alvarado, resident of the río Blanco valley, for logistic support in the field. Chemical analyses and radiometric ages were performed by F. Llona and C. Pérez de Arce respectively, and from the SERNAGEOMIN laboratories. Funding was provided by the Oficina Técnica Puerto Varas (SERNAGEOMIN), and Todos Los Santos Cofrady. Microprobe analyses were funded through the Fondecyt Project number 1020803. E. Córdova

used all his art in producing the final version of the figures. Revisions of the early version of this article by R. Hickey-Vargas (Florida International University, USA), L. López-Escobar (Universidad de Concepción), L. Lara (Servicio Nacional de Geología y Minería) and A. Demant (Université d'Aix Marseille) notably helped to improve the original version. The first author wishes to thank the company, patience and love expressed by Mrs. M. A. Mellado during the long time working on this research.

## **REFERENCES**

Aguirre, L.; Levi, B. 1964. Geología de la Cordillera de los Andes de las provincias de Cautín, Valdivia, Osorno y Llanquihue. *Instituto de Investigaciones Geológicas, Boletín*, No. 17, 37 p. Santiago.

Angermann, D.; Klotz, J.; Reigber, C. 1999. Spacegeodetic estimation of Nazca-South America Euler vector. Earth and Planetary Science Letters, Vol. 171. p. 329-334.

Best, M.; Christiansen, E. 2001. Igneous Petrology. Blackwell Science Inc., 458 p. USA.

Bevis, M.; Isacks, B.L. 1984. Hypocentral trend surface analysis; probing the geometry of Benioff zones.

- Journal of Geophysical Research, Vol. 89, p. 6153-6170.
- Cembrano, J.; Hervé, F.; Lavenu, A. 1996. The Liquiñe-Ofqui fault zone: a long lived intra-arc fault system in southern Chile. *Tectonophysics*, Vol. 259, p. 55-66.
- Clapperton, Ch. 1993. Quaternary Geology and Geomorphology of South America. *Elsevier Publishing Co.*, 779 p. Amsterdam.
- Dessanti, R.N. 1972. Andes Patagónicos Septentrionales. In Geología Regional Argentina (Leanza, A.; editor). Academia Nacional de Ciencias, p. 655-688. Córdoba.
- Duhart, P.; McDonough, M.; Muñoz, J.; Martin, M.; Villeneuve, M. 2001. El Complejo Metamórfico Bahía Mansa en la cordillera de la Costa del centro-sur de Chile (39°30'-42°00'S): geocronología K-Ar, 40Ar/ 39Ar y U-Pb e implicaciones en la evolución del margen sur-occidental de Gondwana. Revista Geológica Chilena, Vol. 28, No. 2, p. 179-208.
- Engebretson, M.J.; Meng, C.I.; Arnoldy, R. L.; Cahill, L. J. 1986. Pc 3 pulsations observed near the south polar cusp. *Journal of Geophysical Research*, Vol. 91 (A8), p. 8909-8918.
- Farmer, G.L.; Broxten, D.E.; Warner, R.G.; Pickthorn, W. 1991. Nd, Sr, and O isotopic variations in metaluminous ash-flow tuffs and related volcanic rocks at the Timber Mountain/Oasis Valley Caldera Complex, SW Nevada, implications for the origin and evolution of largevolume silicic magma bodies. Contributions to Mineralogy and Petrology, Vol. 109, p. 53-68.
- Frey, F.A.; Green, D.H.; Roy, S.D. 1978. Integral models of basaltic petrogenesis: a study of olivine tholeiitic to olivine melilitites from south-eastern Australia utilizing geochemical and experimental petrological data. *Journal of Petrology*, Vol. 9, p. 462-513.
- Futa, K.; Stern, C.R. 1988. Sr and Nd isotopic and trace element compositions of Quaternary volcanic centers of the Southern Andes. *Earth and Planetary Science Letters*, Vol. 88, No. 3-4, p. 253-262.
- Gerlach, D.; Frey, F.; Moreno, H.; López-Escobar, L. 1988. Recent volcanism in the Puyehue-Cordón Caulle region, southern Andes, Chile (40,5°S): Petrogenesis of evolved lavas. *Journal of Petrology*, Vol. 29, p. 333-382.
- Giacosa, R.; Heredia, N. 2001. Hoja Geológica 4172-IV, San Carlos de Bariloche, Provincia de Río Negro y Neuquén. Instituto de Geología y Recursos Minerales, Servicio Geológico Minero Argentino, Boletín, No. 279, 67 p. Buenos Aires.
- Green, D.; Ringwood, A. 1967. The genesis of basaltic magmas. Contributions to Mineralogy and Petrology, Vol. 15, p. 103-190.
- Hickey-Vargas, R.; Gerlach, D.; Frey, F, 1984. Geochemical variations in volcanic rocks from central-south Chile (33°-42°S): implications for their petrogenesis. In Andean magmatism: chemical and isotopic constraints (Harmon R.; Barreiro, B.; editors). Shiva Publishing Limited, p. 72-95. England.
- Hickey-Vargas, R.; Frey, F.A.; Gerlach, D.C.; López-

- Escobar, L. 1986. Multiple sources for basaltic arc rocks from the Southern Volcanic Zone of the Andes (34°-41S): Trace element and isotopic evidence for contributions from subducted oceanic crust, mantle and continental crust. *Journal of Geophysical Research*, Vol. 91, No. 6, p. 5963-5983.
- Hickey-Vargas, R.; Moreno, H.; López-Escobar, L.; Frey, F.A. 1989. Geochemical variations in Andean basaltic and silicic lavas from the Villarrica-Lanin volcanic chain (39.5°S): an evaluation of source heterogeneity, fractional crystallization and crustal assimilation. Contributions to Mineralogy and Petrology, Vol. 103, p. 361-386.
- Köhler, T.P.; Brey, G.P. 1990. Calcium exchange between olivine and clinopyroxene calibrated as geothermobarometer for natural peridotites from 2 to 60 kb with applications. *Geochimica et Cosmochimica Acta*, Vol. 54, p. 2375-2388.
- Lara, L.; Rodríguez, C.; Moreno, H; Pérez de Arce, C. 2001. Geocronología K-Ar y geoquímica del volcanismo Plioceno superior-Pleistoceno de los Andes del sur (39-42°S). Revista Geológica de Chile, Vol. 28, No. 1, p. 67-90.
- Larsson, W. 1940. Petrology of interglacial volcanics from the Andes of Northern Patagonia. Geological Institute, Bulletin, University of Upsala, Vol. 28, p. 191-405.
- Lavenu, A.; Cembrano, J. 1999. Estados de esfuerzos compresivos plioceno y compresivo-transpresivo pleistoceno, Andes del sur, Chile (38°-42°30'S). Revista Geológica de Chile, Vol. 26, No. 1, p. 67-87.
- Ljungner, E. 1931. Geologische Aufnahmes in der Patagonischer kordillera. University of Upsala, Geological Institute, Bulletin, Vol. 23, p. 203.
- López-Escobar, L.; Frey, F.A.; Vergara, M. 1976. Andesites from central-south Chile: Trace elements abundances and Petrogenesis. In IAVCEI Proceedings of the Symposium on Andean and Antarctic Volcanology Problems (González-Ferrán, O.; editor), p. 725-761.
- López-Escobar, L.; Frey, F.; Vergara, M. 1977. Andesites and high alumina basalts from the central-south Chile High Andes: geochemical evidences bearing on their petrogenesis. Contributions to Mineralogy and Petrology, Vol. 63, p. 199-228.
- López-Escobar, L.; Parada, M.A.; Moreno, H.; Frey, F.A.; Hickey-Vargas, R.L. 1992. A contribution to the petrogénesis of Osorno and Calbuco volcanoes, Southern Andes (41°00'-41°30'S): comparative study. Revista Geológica de Chile, Vol. 19, No. 2, p. 211-226.
- López-Escobar, L.; Kilian, R.; Kempton, P.; Tagiri, M. 1993. Petrography and geochemistry of Quaternary rocks from the Southern Volcanic Zone between 41°30' and 46°00'S, Chile. Revista Geológica de Chile, Vol. 20, No. 1, p. 35-55.
- López-Escobar, L.; Kempton, P.D.; Moreno, H.; Parada, M.A.; Hickey-Vargas, R.; Frey, F.A. 1995a. Calbuco volcano and minor eruptive centers distributed along

- the Liquiñe-Ofqui fault zone, Chile (41°-42°S): contrasting origin of andesitic and basaltic magma in the Southern Volcanic Zone of the Andes. *Contributions to Mineralogy and Petrology*, Vol. 119, p. 345-361.
- López-Escobar, L.; Cembrano, J.; Moreno, H. 1995b. Geochemistry and tectonics of the Chilean Southern Andes basaltic Quaternary volcanism (37°-46°S). Revista Geológica de Chile, Vol. 22, No. 2, p. 219-234.
- Lowrie. A.; Hey, R. 1981. Geological and geophysical variation along the western margin of Chile near lat. 33° to 36°S and their relation to Nazca plate subduction. Geological Society of America, Memoir, Vol. 154, p. 741-754.
- McMillan, N.J.; Harmon, R.S.; Moorbath, S.; López-Escobar, L.; Strong, D.F. 1989. Crustal sources involved in continental arc magmatism: a case study of volcan Mocho-Choshuenco, southern Chile. *Geology*, Vol. 17, p. 1152-1156.
- Mella, M.; Muñoz, J.; Vergara, M.; Belmar, M. 2003a. 'Fibro-Palagonita' en basaltos del Complejo Volcánico Tronador (CTV), Andes del Sur (41°S), Chile. In Congreso Geológico Chileno, No. 10, Actas, CD-ROM, Sesión Temática, No. 5. Concepción.
- Mella, M.; Muñoz, J.; Vergara, M.; Klohn, E. 2003b. Hidrovolcanismo Pleistoceno en el complejo Volcánico Tronador, Zona Volcánica Sur (41°S). In Congreso Geológico Chileno, No. 10, Actas, CD-ROM, Sesión Temática 5. Concepción.
- Mercer, J.H. 1976. Glacial history of southern South America. *Quaternary Research*, Vol. 6, p.125-166.
- Moreno, H.; Parada, M.A. 1976. Esquema geológico de la cordillera de los Andes entre los paralelos 39°00' y 41°30'S. *In Congreso Geológico Chileno, No. 1, Actas,* Vol. 1, p. A213-A225. Santiago.
- Moreno, H.; Naranjo, J.A.; López-Escobar, L. 1979. Geología y petrología de la cadena volcánica Osorno-Puntiagudo, Andes del Sur, Latitud 41°-10'S. In Congreso Geológico Chileno, No. 2, Actas, Vol. 3, p. E109-E131. Arica.
- Muñoz, J.; Stern, C.R. 1988. The Quaternary volcanic belt of the southern continental margin of South America: transverse structural and petrochemical variations across the segment between 38°S and 39°S. Journal of South American Earth Sciences, Vol. 1, p. 147-161.
- Muñoz, J.; Stern, C.R. 1989. Alkaline magmatism within the segment 38-39°S of the Plio-Quaternary volcanic belt of the southern South American continental margin. *Journal of Geophysical Research*, Vol. 94, p. 4545-4560.
- Peccerillo, A.; Taylor, S.R. 1976. Geochemistry of Eocene calc-alkaline volcanic rocks from the Kastamonu area, Northern Turkey. Contributions to Mineralogy and Petrology, Vol. 58, p. 63-81.
- Porter, S.C. 1981. Pleistocene glaciation in the southern lake district of Chile. *Quaternary Research*, Vol. 16,

- p. 263-292
- Rabbasa, J.; Evenson, C. 1986. Reinterpretación de la estratigrafía glaciaria de la región de San Carlos de Bariloche (provincia de Río Negro, Argentina). In Congreso Geológico Argentino, No. 13, Actas, Vol. 4, p. 327, Buenos Aires.
- Rabbasa, J.; Clapperton, C. 1990. Quaternary glaciations in southern Andes. *Quaternary Science Reviews*, Vol. 9, p. 153-174.
- Rabassa, J.; Evenson, C.; Schlieder, G.; Clinch, J.M.; Stephens, G.; Zeitler, P. 1987. Edad Pre-Pleistoceno superior de la glaciación El Cóndor, valle del río Malleo-Neuquén. República Argentina. *In Congreso Geológico Argentino*, No.10, *Actas*, Vol. 3, p. 261-263. Buenos Aires.
- Rollinson, H.R. 1993. Using Geochemical Data: Evaluation, Presentation, Interpretation. Longman Group Limited, 352 p. United Kingdom.
- Servicio Nacional de Geología y Minería-Bureau de Recherches Géologiques et Minieres (SERNAGEO-MIN-BGRM). 1995. Carta metalogénica de la Xa Región Sur. Servicio Nacional de Geología y Minería-Bureau de Recherches Géologiques et Minieres. Informe Registrado, IR-95-05, 4 Tomos, 10 Vols., 95 mapas. Santiago.
- Servicio Nacional de Geología y Minería (SERNAGEO-MIN), 1998. Estudio Geológico-Económico de la X Región Norte, Chile. Servicio Nacional de Geología y Minería, Informe Registrado, IR-98-15, Vol. 2, 244 p. Santiago.
- Sheridan, M.; Wohletz, K.H. 1983. Hydrovolcanism: basic considerations and review. *Journal of Volcanology* and Geothermal Research, Vol. 17, p. 1-29.
- Steffen, H. 1910. Viajes de Esploracion i Estudio en la Patagonia Occidental:1892-1902. Anales de la Universidad de Chile, Imprenta Cervantes, 2 Vol. Santiago.
- Steffen, H. 1947. Patagonia Occidental. Las Cordilleras Patagónicas y sus regiones circundantes. Ediciones de la Universidad de Chile, Vol. 1, p. 333. Santiago.
- Stern, C.R. 1988. Source region versus intra-crustal contamination in the petrogenesis of the Quaternary volcanic centers at the northern end (33-34° S) of the Southern Volcanic Zone. In Congreso Geológico Chileno, No. 5, Actas, Vol.3, p. 129-145. Santiago.
- Stern, C.R. 1989. Pliocene to Present migration of the volcanic front, Andean Southern Volcanic Zone. Revista Geológica de Chile, Vol. 16, No. 2, p. 145-162.
- Stern, C.R. 1991. Role of subduction erosion in the generation of the Andean magmas. *Geology*, Vol. 19, p. 78-81.
- Stern, C.R. 2004. Active Andean volcanism: its geologic and tectonic setting. Revista Geológica de Chile, Vol. 31, No. 2, p. 161-206.
- Stern, C.R.; Skewes, M.A.; Duran, M. 1976. Volcanismo Orogénico en Chiloé Austral. In Congreso Geológico de Chile, No. 1, Actas, Vol. 2, p. 195-212. Santiago.

Stern, C.R.; Frey, F.A.; Futa, K.; Zartman, R.E.; Peng, Z.; Kyser, K.T. 1990. Trace element and Sr, Nd, Pb, and O isotopic compositions of Pliocene and Quaternary alkali basalts of the Patagonian Plateau lavas of southernmost South America. Contributions to Mineralogy and Petrology, Vol. 104, p. 294-308.

Sun, S.; McDonough W.F. 1989. Chemical and isotopic

systematic of oceanic basalt: implications for mantle composition and processes. In Magmatism in the ocean basis (Saunders A.D.; Norry, M.J.; editors). Geological Society, Special Publication, No. 42, p. 313-345.

Tatsumi, Y.; Eggins, S. 1995. Subduction Zone Magmatism. Blackwell Science, 211 p. Cambridge.

Manuscript received: November 21, 2003; accepted: December 3, 2004